THESIS

BIOMECHANICAL ANALYSIS OF AORTIC VALVE CALCIFICATION AND POST-PROCEDURAL PARAVALVULAR LEAK

Submitted by

Banafsheh Zebhi

Department of Mechanical Engineering

In partial fulfillment of the requirements

For the Degree of Master of Science

Colorado State University

Fort Collins, Colorado

Spring 2016

Master's Committee:

Advisor: Lakshmi Prasad Dasi

Christopher Orton
Xinfeng Gao

ABSTRACT

BIOMECHANICAL ANALYSIS OF AORTIC VALVE CALCIFICATION AND POST-PROCEDURAL PARAVALVULAR LEAK

Cardiovascular disease is a leading cause of death accounted for 17.3 million people annually. Aortic valve calcification (AVC) and stenosis are the most common diseases among valvular heart diseases. Severe AVC and stenosis will need the standard surgical aortic valve replacement (SAVR) or transcatheter aortic valve replacement (TAVR) for patients who are at high risk for open heart surgery. Post-procedural paravalvular leak (PVL) is a common complication which occurs around the implanted stent in a significant population of patients who undergo valve replacement, requiring significant interventions. The overarching hypothesis of this research is that anatomic characteristics of patients' native aortic valve play an important role in both calcification processes and post-procedural PVL occurrence. This hypothesis is studied through two specific Aims. Aim 1 was designed to determine what anatomic and biological parameters as well as hemodynamic factors are associated with severity of aortic valve calcification. In this aim, patient-specific geometric characteristics were extracted using 3D image reconstruction of patient CT data, and their relation with cusp specific calcification was evaluated using multiple regression analysis. The results of this analysis indicated that severity of calcification is significantly correlated with coronary calcification as well as the size of sinus of valsava and sinotubular junction (all p-values<0.05). In Aim 2, we investigated the relationship among patients' calcification level and anatomic parameters of their native aortic valve as well as the risk of post-procedural PVL occurrence. Using a logistic regression analysis

model we show that large calcification deposition (p-value<0.001) and large ratio of sinus of valsava to annulus (p-value<0.02) of native aortic valve can predict probability of post-procedural PVL occurrence. The overall significance of this study is that bioengineering analysis of pre-procedural CT data can be utilized towards better TAVR planning as well as basic understanding of the pathogenesis of AVC.

ACKNOWLEDGENTS

I would like to express my gratitude to whom supported me during my graduate education and contributed in my research. First and foremost, I would like to acknowledge my advisor, Dr. Prasad Dasi for his valuable advice and knowledge in leading this research project. I greatly appreciate Dr. Dasi for giving me the chance to work with him. I would like to extend my thanks to my committee members, Dr. Christopher Orton and Dr. Xinfeng Gao.

I am grateful to Dr. Gary Luckasen for collaborating in this research. I particularly thank Joel Klitch for consistently taking time to share patients' data and clinical information with our lab.

I would like to thank Mechanical Engineering Department for supporting me through a Graduate Teaching Assistantship.

I am grateful to my fellow graduate students in the Cardiovascular and Biofluid Mechanics Laboratory especially Brandon Moore who greatly guided me in biomechanics concept of this research. I would also like to thank undergraduate student, Cristian Bueno who assisted me in image processing of this research.

Last but not least, I greatly appreciate my parent for supporting and encouraging me during the entire period of my education as well as Mohammadreza Gorakhki whom was a great motivation during my master's education.

TABLE OF CONTENTS

LIST OF FIGURES

1. INTRODUCTION

Cardiovascular disease is a leading cause of death accounted for 17.3 million people annually (Alwan 2011). Aortic valve calcification (AVC) and stenosis are the most common diseases among valvular heart diseases which increase by aging (Lindroos, Kupari et al. 1993; Mohler III 2004). According to 2015 report of American Heart Association (AHA), prevalence of valvular disease increases by 13.3% in people older than 75 (Mozaffarian, Benjamin et al. 2015). Surgical aortic valve replacement (SAVR) in low-risk young patients and transcatheter aortic valve implantation (TAVI) in elderly patients with higher risk for surgery are two common treatments for aortic stenosis. However, paravalvular leak (PVL) remains as a common complication around the implanted stent in a significant population of patients after treatment (Colli, D'Amico et al. 2011). Therefore, several studies have been performed to determine the risk factors associated with calcification of aortic valve and post-procedural PVL (Abdel-Wahab, Zahn et al. 2011; Kodali, Pibarot et al. 2014).

Arterial and valvular calcification has been studied from biological and biomechanical prospective over the past decades. At the molecular scale, mush efforts have been made to explain the initiation of calcification (Aikawa, Nahrendorf et al. 2007; Otto 2008; Hjortnaes, New et al. 2013). Previous studies suggested that calcification of cardiovascular system is similar to formation of bone (Mohler, Gannon et al. 2001; Rajamannan, Subramaniam et al. 2003). Calcification initiates with inflammation and leads to mineralization (Freeman and Otto 2005). Studies performed on hemodynamic of aortic valve at macroscopic and microscopic scales, show that stress and strain around the aortic valve play an important role in calcification

of aortic valve disease (Gould, Srigunapalan et al. 2013). Aortic valve fluid shear stress activates endothelial cells by elongation and realignment of cells. Bending stress rises during the opening and closing the valve leaflets. High shear and bending stresses in the leaflets is associated with calcification of the leaflets (Balachandran, Sucosky et al. 2011).

Other studies have shown that metabolic syndromes such as blood sugar, cholesterol level and hypertension as well as age, sex and body mass index (BMI) may also affect AVC (Lindroos, Kupari et al. 1994; Katz, Wong et al. 2006). Some studies suggested that age, BMI and hypertension increases the likelihood of AVC (Lindroos, Kupari et al. 1994). Similar investigations indicated that female sex and diabetes were also associated with AVC (Boon, Cheriex et al. 1997). It has been suggested that high level of LDL cholesterol (LDL > 130 mg/dL) increases both coronary and aortic valve calcification progress (Demer 2001; Pohle, Mäffert et al. 2001). Clinical studies have shown that chronic renal disease (CRD) is associated with calcification since 50% of the patients with CRD die due to arterial and valvular calcification (Schiffrin, Lipman et al. 2007; Aikawa, Aikawa et al. 2009).

More recent studies confirmed that location and severity of aortic valve calcification are associated with PVL, since degree of calcification in patients with PVL was significantly higher than calcification score in patients without PVL (Grünenfelder and Emmert 2015; Koh, Lam et al. 2015). Previous study suggests that longer ascending aorta and arch are related to occurrence of post–procedural PVL (Nemoto, Rutten-Ramos et al. 2014). Additionally, the size of annulus, degree of aortic stenosis and pre-TAVI aortic regurgitation were also predictors of PVL (Takagi, Latib et al. 2011). Small left ventricle ejection fraction (LVEF) and diabetes were reported to be related to post-procedural mortality (Tamburino, Capodanno et al. 2011). Post-TAVI aortic regurgitation (AR) increases with increasing angle of left ventricular outflow tract to ascending

aorta (Sherif, Abdel-Wahab et al. 2010). It also appeared that commissural calcification between right coronary and non-coronary cusps were independent predictors of post-procedural PVL (Gripari, Ewe et al. 2012).

The overarching hypothesis of this research is that anatomic characteristics of patients' native aortic valve play an important role in both calcification processes and post-procedural PVL occurrence. This hypothesis is studied through two specific Aims. Aim 1 was designed to determine what anatomic and biological parameters as well as hemodynamic factors are associated with severity of aortic valve calcification. In this aim, calcification depositions in patient's CT scans were segmented using a 3D model reconstructing tool. The patient-specific geometric characteristics as well as hemodynamic and biological factors were extracted from patient's database and their relation with cusp specific calcification was evaluated using multiple regression analysis. In Aim 2, we investigated the relationship among patients' calcification level and anatomic parameters of their native aortic valve as well as the risk of post-procedural PVL occurrence.

This thesis is represented in five chapters. Chapter 1 is the introduction to this study. Chapter 2 includes anatomy and physiology of heart and aortic valve as well as heart valve disease, calcification mechanism and possible treatment approaches; Chapter 3 and 4 covers Aim 1 and Aim 2, respectively. In each chapter applied methodologies, results and discussion of each experiment are presented and Chapter 5 is a summary of the investigation.

2. BACKGROUND

This chapter is an overview of anatomical and physiological structure of human heart. In sections 2.1 and 2.2 anatomy and physiology of heart and aortic valves are explained; in section 2.3 hemodynamic and mechanobiology of calcification mechanism are discussed; and at the end of the chapter, in section 1.4, heart valve diseases that are caused by calcification along with artificial heart valves as treatments for calcification disease are discussed.

2.1 Heart

2.1.1 Anatomy of Heart

The heart is a muscular organ in humans and most of animals, which is located between lungs and provides organs with nutrient through the circulatory system. The human heart consists of four chambers. Two upper chambers are right and left atrium and two lower chambers are right and left ventricles. There are four valves through which blood passes before leaving each chamber of the heart. The heart valve acts as a one-way inlet that allows blood to flow from atrium to ventricle or from ventricle to atrium. The valves prevent the backward flow of blood. The four heart valve include; tricuspid valve which is located between right atrium and right ventricle, pulmonary valve which is located between right ventricle and pulmonary artery, mitral valve which is located between left atrium and left ventricle and aortic valve which is located between left ventricle and aorta. The tricuspid, pulmonary and aortic valves have three leaflets while the mitral valve has two leaflets. The four chamber and the valves are shown in Figure 2.1.

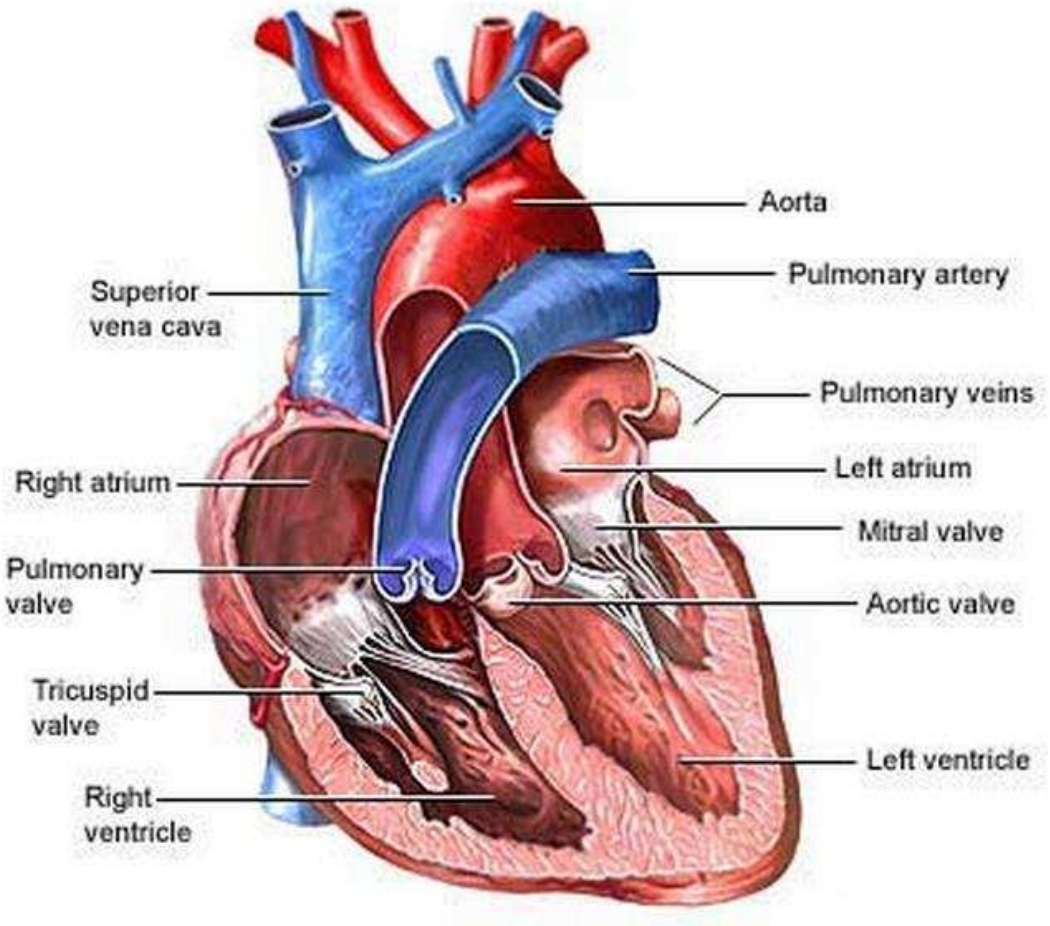

Figure 2.1. Anterior sagittal view of human heart showing anatomical position of chambers and valves. The figure is adapted from http://www.nytimes.com

2.1.2 Physiology of Heart

In the circulatory system, right atrium collects the deoxygenated blood from body through superior vena cava and pumps it to right ventricle. Deoxygenated blood in the right ventricle is then pumped to lungs via pulmonary arteries. In the pulmonary circulation through the lungs, deoxygenated blood receives oxygen and loses metabolic wastes. The oxygenated blood returns to left atrium and left ventricle through pulmonary veins. In the left ventricle, high pressure pumps out oxygenated blood into organs of the body via the circulatory system.

Circulation occurs through two cardiac cycles includes systole and diastole. Systole refers to the moments that ventricles contract and pumps out the blood while diastole is when ventricles are relaxed and refills with blood. The top section of Figure 2.2 shows electrocardiographic signal of the heart which is generated at different moments of systole and diastole cycles. The pressure changes in left atrium, left ventricle and aorta regions during atrial and ventricular systole and diastole is depicted in the middle of the diagram. The bottom of the diagram shows accumulated blood volume in left ventricle during the cycles.

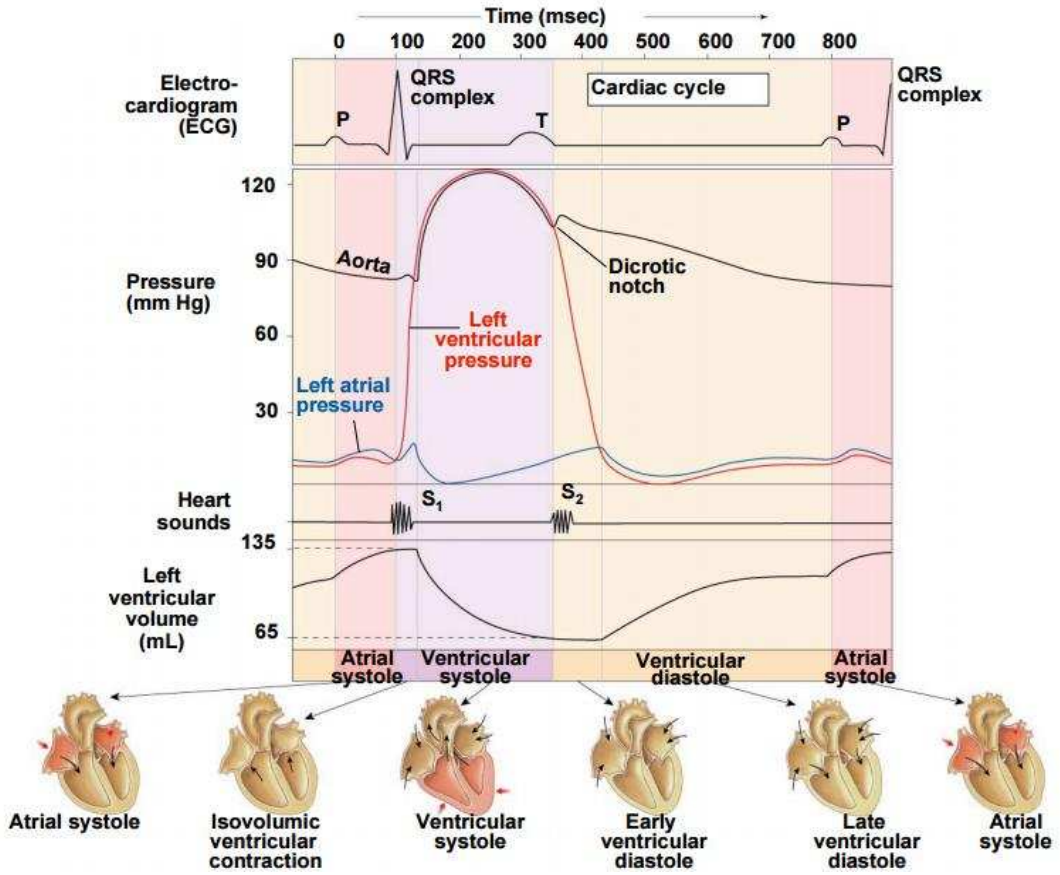

Figure 2.2. The Wigger's diagram indicates the normal cardiac pressure and volume at specific moment of cardiac cycle. The diagram is adapted from http://intranet.tdmu.edu.ua

As can be seen in Figure 2.2, cardiac cycle occurs in 5 stages; (1) late diastole: when both right and left chambers are relaxed and ventricles fill with blood. (2) Atrial systole pumps small

amount of blood into ventricles. (3) Isomeric ventricular contraction which increases internal pressure of ventricle to open heart valve. (4) Ventricular systole open the valves and pump out blood with high pressure. (5) Isomeric ventricle relaxation drops the pressure inside the ventricles so they can refill in next stage (http://www.medicine.tcd.ie/physiology).

2.2 Aortic Valve

2.2.1 Anatomy of Aortic Valve

Aortic valve consist of three semilunar cusps and three leaflets. The three cusps are named according to their anatomical positions. The cusps near the right and left chambers are named right and left coronary cusp. Right coronary artery exits from right coronary cusp to supply blood into right atrium and right ventricle as well as bottom portion of both ventricles and back of the septum (http://my.clevelandclinic.org). Similar to right coronary artery, left coronary artery exit from associated cusp and divides two branches of circumflex artery and left anterior descending artery to provide nutrient for left atrium and left ventricle as well as bottom of left ventricle and front of septum (http://my.clevelandclinic.org). The other cusp is named non-coronary cusp due to lack of the coronary artery. Figure 2.3 shows the anatomical position of aortic valve and three leaflets.

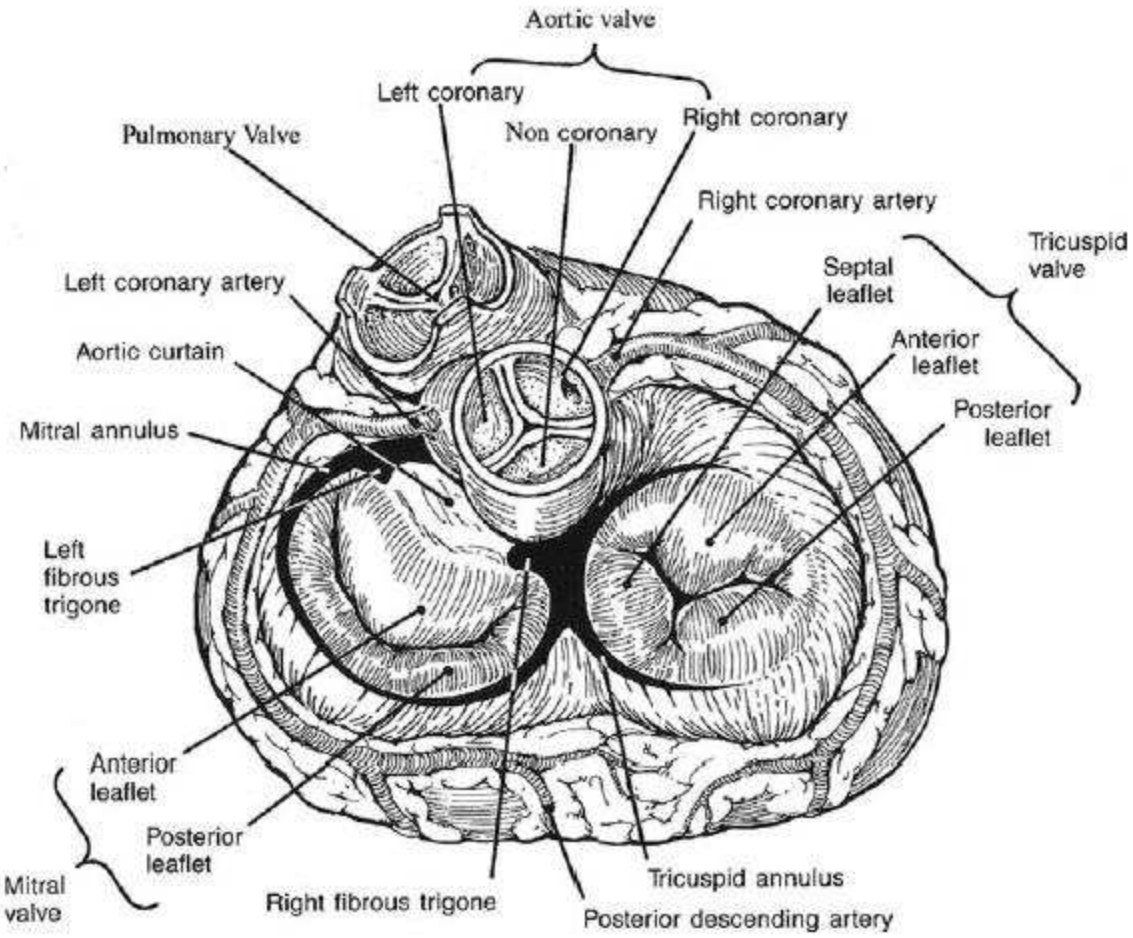

Figure 2.3. Short axis view of the four heart valve; aortic valve, mitral valve pulmonary and tricuspid. Aortic valve with three leaflets is located in the middle of other three valves (Iaizzo 2009)

Figure 2.4 shows a schematic of an aortic valve which has been open from commissure line between right and left coronary sinuses.

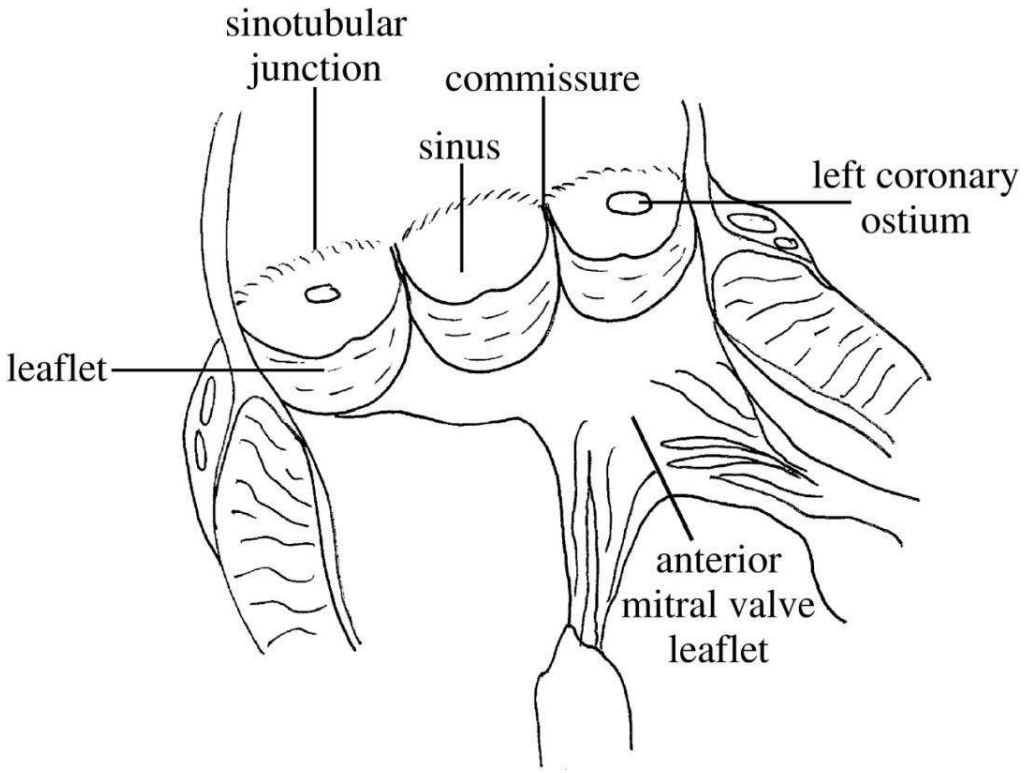

Figure 2.4. Schematic of aortic valve showing right coronary, non-coronary and left coronary cusps from left to right. The cusps are attached at the commissures. Left and right coronary astiums are across the non-coronary sinus (Misfeld and Sievers 2007)

2.2.2 Dynamics of Aortic valve

At the beginning of the ventricle systole, aortic valve opens and blood flow accelerates and before beginning of the ventricle diastole, it closes and blood flow decelerates (Balachandran, Sucosky et al. 2011). Systolic cycle begins with opening of the aortic valve and lasts about one third of the cardiac cycle. In the systolic cycle, when valve is fully open, velocity of blood flow reaches the peak then decreases rapidly and aortic pressure gradually increases and reaches 120 mm Hg in normal people (Yoganathan, He et al. 2004). Near the end of the systolic phase before valve is fully closed little backward flow enters ventricles. Figure 2.5 shows pressure and flow changes during systolic and diastolic cycles. At the end of systole, adverse pressure and low

inertia flow create vortices in sinuses which force the leaflet belly toward the ventricle and close the valve (Reul and Talukder 1979).

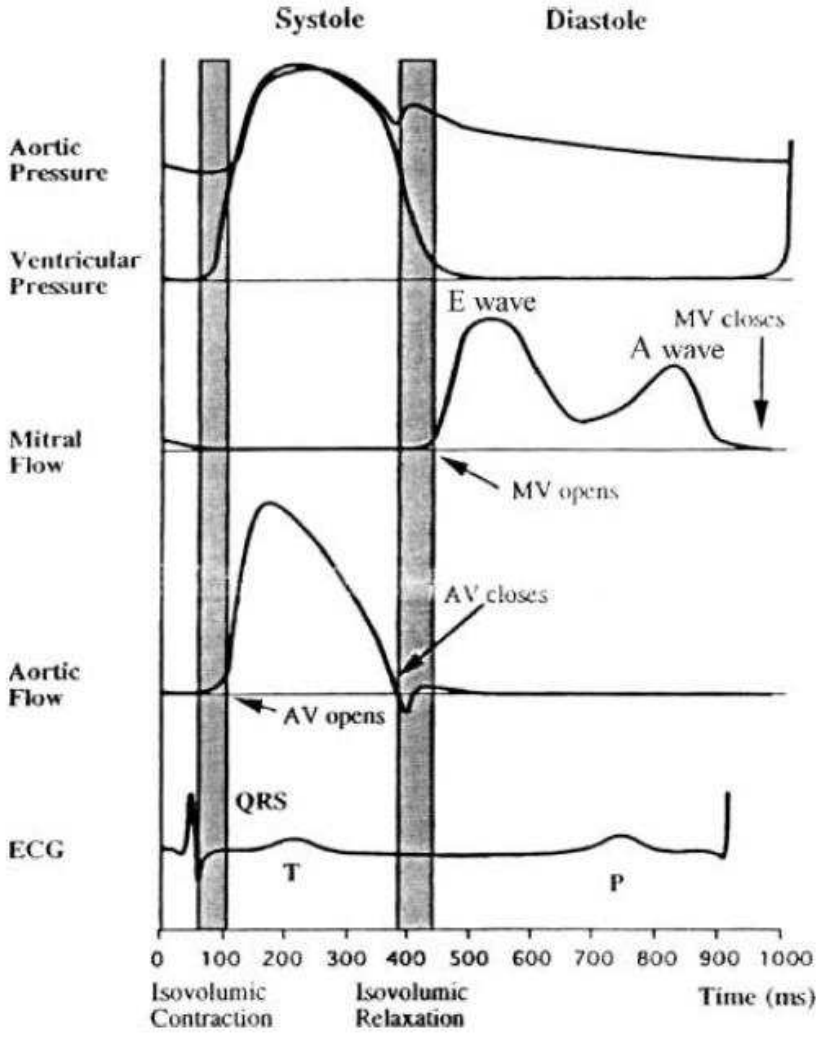

Figure 2.5. Pressure and flow changes during the systolic and diastolic cycles (Yoganathan, He et al. 2004)

2.3 Hemodynamics and Mechanobiology of Aortic Valve Calcification

It has been investigated that diseases of cardiovascular system are often associated with metabolic disorders (Aikawa, Manabe et al. 2012) and inflammation is the main cause of metabolic cardiovascular diseases which leads to aortic valve calcification and aortic valve stenosis (Aikawa, Manabe et al. 2012). Inflammation occurs due to dysfunction of two types of cells (1) endothelial cells that are located on the surface of the aortic valve cusps and (2) interstitial cells in the body of the valve (Balachandran 2010). The roles of endothelial cells are to maintain normal homeostasis at the interface of blood with cusp vasculature (Hjortnaes, New et al. 2013) and provide nutrient for interstitial cells in the body of valve (Freeman and Otto 2005; Butcher and Nerem 2007). Calcification of aortic valve initiates with dysfunction of endothelial cells and inflammation and leads to mineralization. Calcification begins with activation of endothelial cells and via activation of phenotypes of interstitial cells leads to mineralization (Figure 2.6).

Studies performed on hemodynamic in aortic valve at macroscopic and microscopic scales, show that force and pressure around the aortic valve play an important role in calcification of aortic valve disease (Watanabe, Lefèvre et al. 2015). From the macroscopic scale prospective, hemodynamic forces deform the leaflets of the valve and will be transduced to microscale forces (Watanabe, Lefèvre et al. 2015). Microscale forces influence endothelial and interstitial cells in extracellular matrix of the valve (Watanabe, Lefèvre et al. 2015). Figure 2.6 shows the structure of aortic valve in macroscopic and microscopic scales. Fibrosa layer is located on the aortic side of the valve and aligned circumferentially (2.7 C). Sponginosa layer is the middle layer and located between fibrosa and ventricularis. Sponginosa provide smooth motion for opening and

closing the leaflet. Ventricularis layer is on the ventricular side and makes leaflet flexible to move (Watanabe, Lefèvre et al. 2015).

It has been reported that hemodynamic forces regulate vascular interstitial cells (VIC) function (Jilaihawi, Kashif et al. 2012). Stretch of aortic valve tissue during the cardiac cycles makes leaflets to lengthen circumferentially and radially (Balachandran, Sucosky et al. 2011). Anisotropic force and stretch of valve leaflets affect valve function as well as mechanobiolgical responses of vascular interstitial cells (Marom, Halevi et al. 2013). Since fibrosa is stiffer than ventricularis (Merryman, Huang et al. 2006; Mirnajafi, Raymer et al. 2006), it is more influenced by strain therefore interstitial cells in the fibrosa deform more than those in ventricularis layer (Huang, Liao et al. 2007). This explains formation of calcification in fibrosa layer of the valve (Yip and Simmons 2011) (see Figure 2.7).

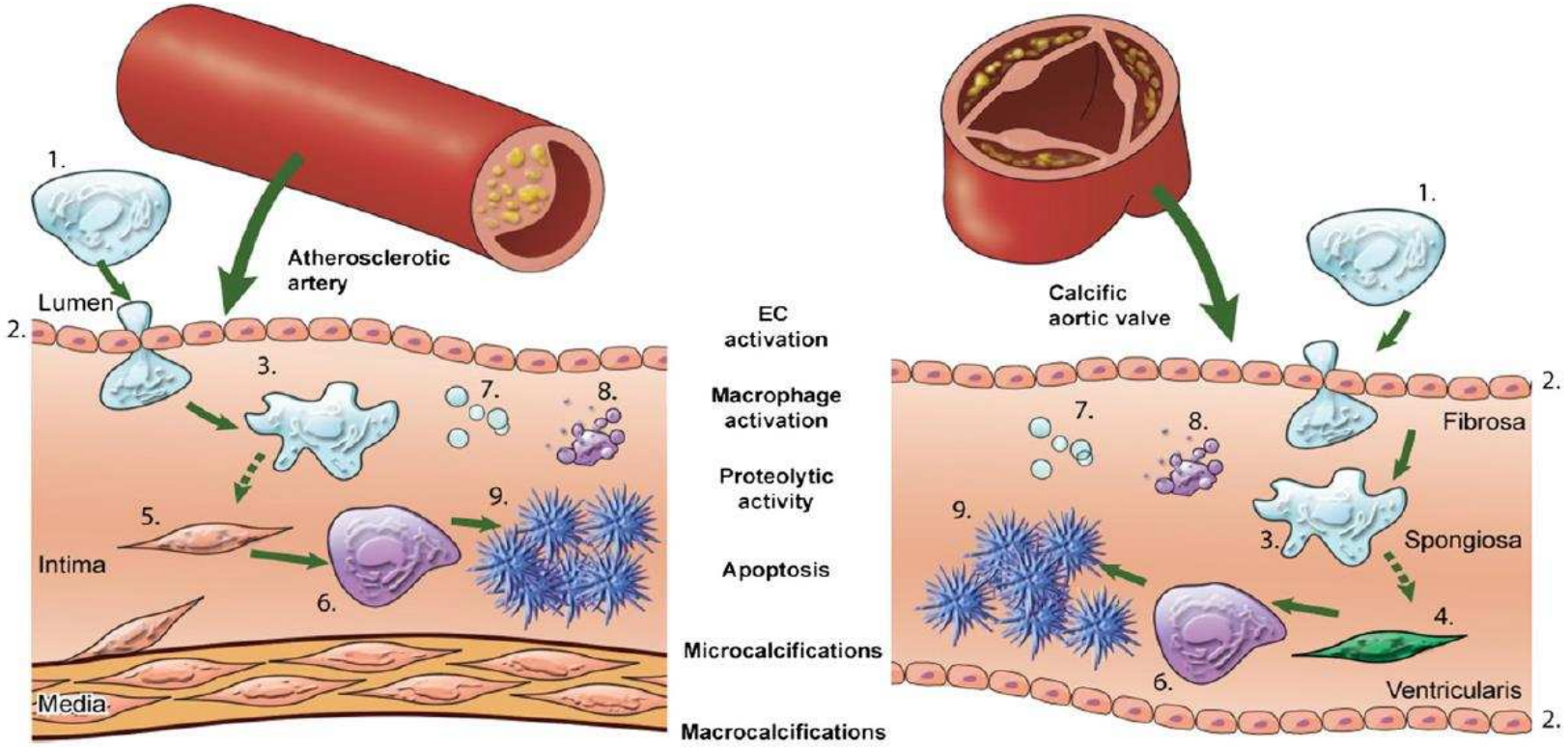

Figure 2.6. Schematic of mechanism of arterial and valvular calcification. Monocytes (1) are placed on the aortic site of the valve due to the activation of endothelial cells (EC). (2) Activated/damaged EC increases expression of adhesion molecule VCAM-1 and leads to macrophage activation (3). Macrophages release proteolytic enzymes to stimulate myofibroblasts (4) and smooth muscle (5) to differentiate into osteoblasts. Formation of osteoblast (6) and microcalcification results in formation of a calcified matrix vesicle (7) and apoptosis (8). Activities of mentioned components lead to calcification (9) on the aortic side of the valve (Zarayelyan 2015)

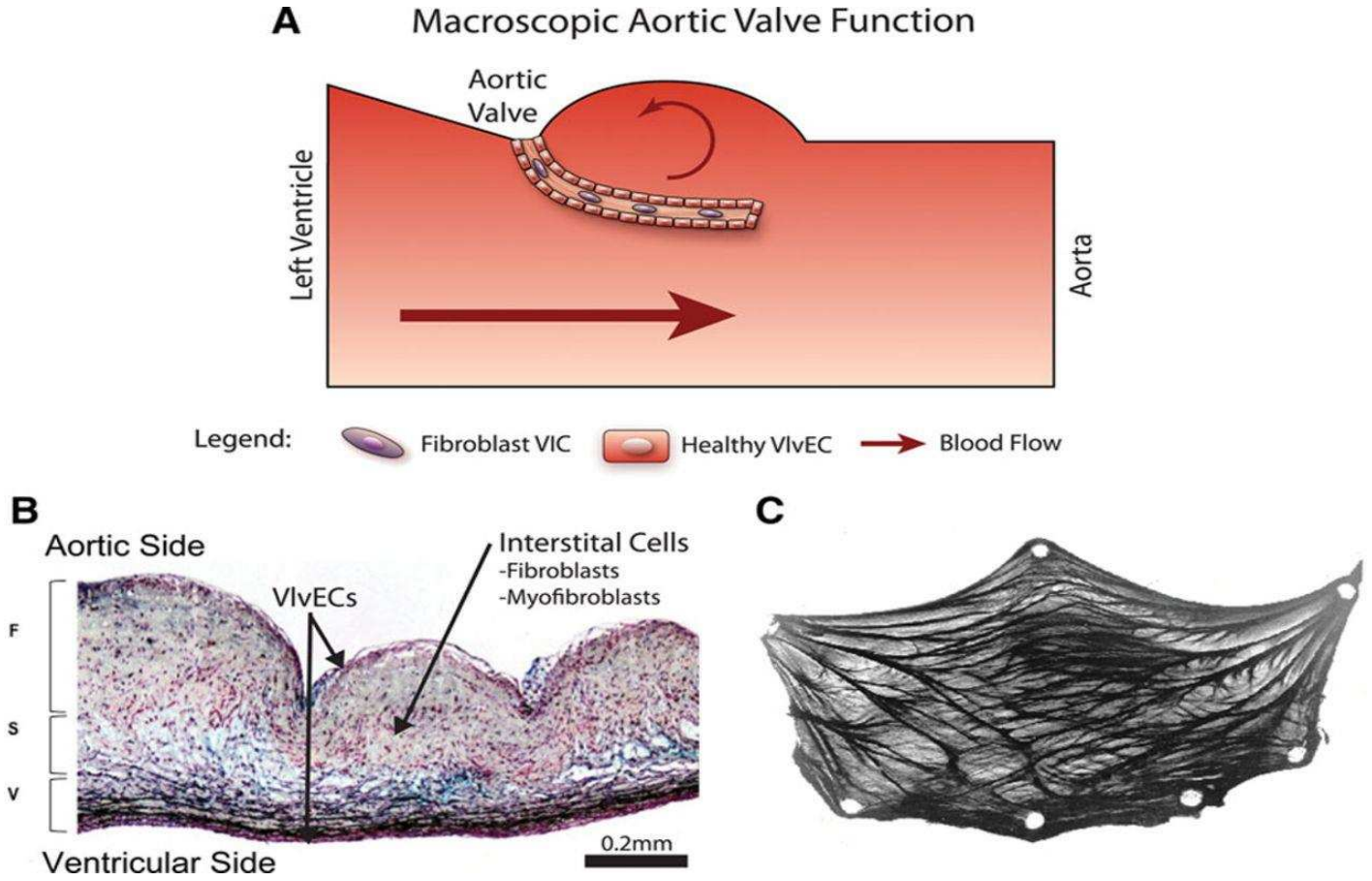

Figure 2.7. Schematic of coronary sinus of aortic valve (B) The histological view of aortic valve leaflet has three layers of fibrosa [F], spongiosa [S], ventricularis [V] (Watanabe, Lefèvre et al. 2015). (C) View of fiber architecture on an aortic valve leaflet. Fibers are mostly distributed circumferentially (Willson, Webb et al. 2012)

2.4 Aortic Valve Disease

Although all four valves and many regions of human cardiovascular system are affected by disease, the only disease that is discussed in this section is aortic valve calcification disease.

2.4.1 Aortic Valve Stenosis and Regurgitation

One of the most common diseases of aortic valve is aortic stenosis which narrows the opening of the valve and prevent valve from opening fully which causes blood to flow forward during the systolic period. The most common cause of aortic stenosis is formation of calcium deposition (calcification) on the valve leaflets (Iaizzo 2009). Calcification starts with inflammation and develops by aging (Hjortnaes, New et al. 2013) which was briefly explained in previous section. As aortic valve calcification disease progresses leaflets of the valve become thicker and stiffer (Iaizzo 2009). Aortic stenosis causes regurgitation which occurs when valve doesn't close tightly and blood flows back to the ventricle during the diastolic period (Iaizzo 2009).

Color-flow Doppler echocardiography is a common clinical method to assess the severity of valve stenosis and regurgitation. In a color-flow Doppler echocardiograph blood flow velocity is measured in a 2D environment. In Figure 2.8 red and blue colors indicate the direction of blood flow passing through heart valve in an echo image. In color-flow Doppler echocardiography red color is assigned to the flow that moves toward the transducer and blue color is assigned to the flow that goes away from transducer. Color-flow Doppler image enables physicians to diagnose stenosis and regurgitation by evaluating the direction of blood flow.

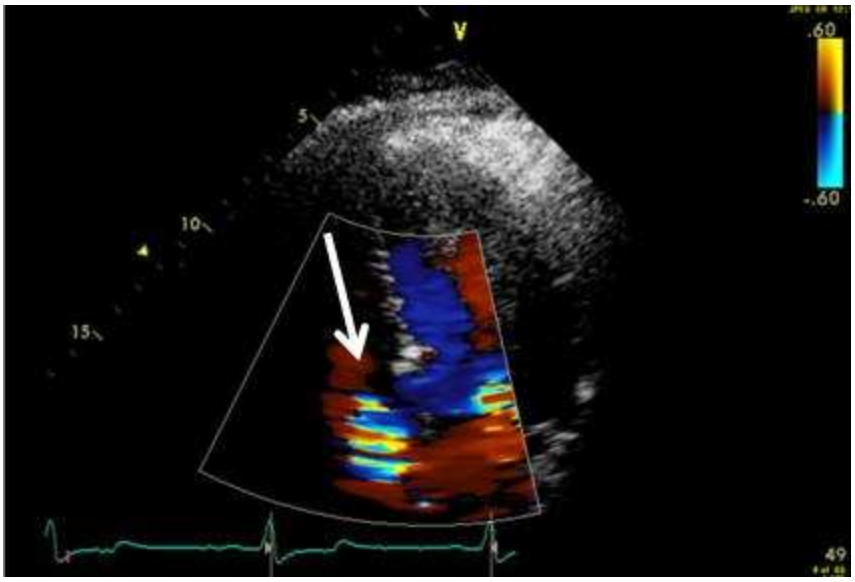

Figure 2.8. Color flow Doppler display of tricuspid valve regurgitation (Sorrell and Kumar 2011). The arrow indicates backward flow

Severity of aortic disease can be defined by mean pressure gradient, aortic jet velocity and valve orifice area (Iaizzo 2009). Table 2 indicates severity of stenosis in three categories defined by Iaizzo.

Table 2.1 Degree of aortic stenosis (Iaizzo 2009)

Stenosis	Valve Orifice area (mm^2)	Peak Aortic Velocity (m/s)
Mild	> 1.5	< 3.0
Moderate	> 1.0-1.5	3.0 -4.0
Severe	<1.0	> 4.0

2.4.2 Artificial Heart Valve

It has been reported that 492,042 people die annually because of rheumatic heart disease (Carapetis, Steer et al. 2005). Development of heart diseases has been led to artificial heart valve design and cardiac valve replacement. Artificial heart valves can be categorized in 2 major types; mechanical prosthetic valves and biological prosthetic (bioprosthetic) valves (Dasi, Simon et al. 2009; Iaizzo 2009). In 1952, the world first successful mechanical heart valve designed by Dr. Charles Hufnagel was implanted into human body (Hufnagel 1950) (Figure 2.9). Since then,

more than 50 artificial heart valve designs have been developed (Dasi, Simon et al. 2009). Over the decades, mechanical heart valve designs have been developed and tilting-disc valve and bileaflet mechanical heart valve are generated. In 1969 and 1970, tilting-disc valve was introduced by Bjork-Shiley and Lillehei-Kaster (Björk 1969; Kaster, Lillehei et al. 1970) (Figure 2.10) and in 1978, bileaflet heart valves were designed and presented by St Jude Medical (SJM) Inc. (Minneapolis, MN, USA) (Possis 1978) (Figure 2.11).

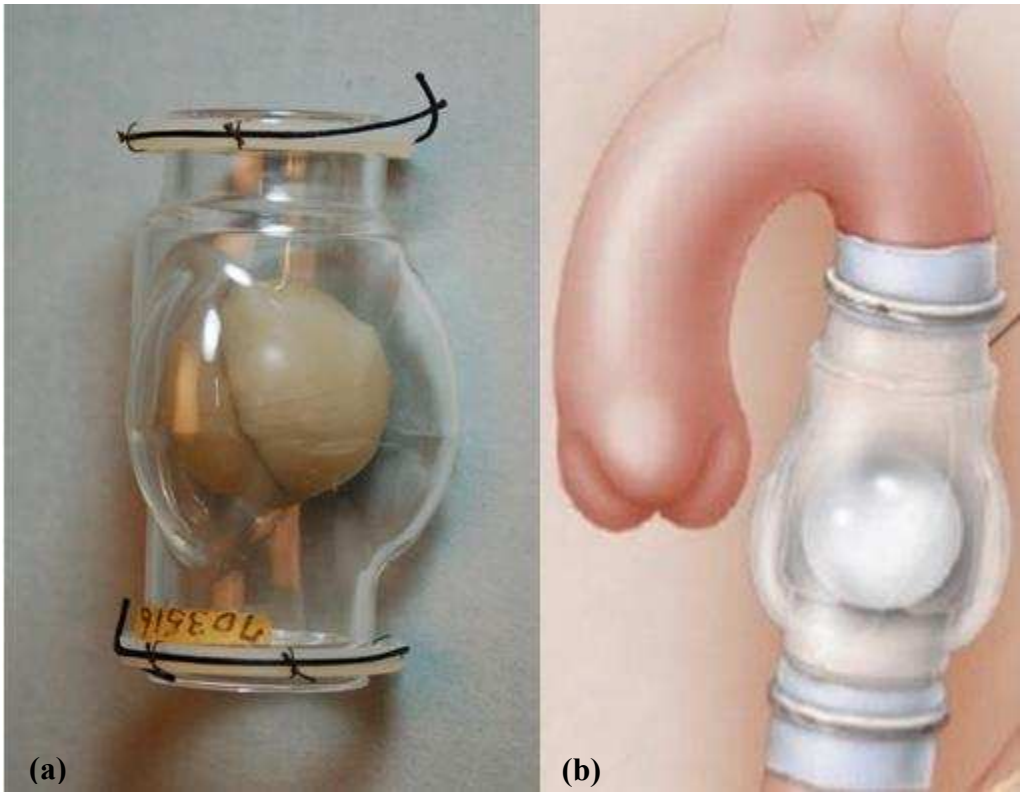

Figure 2.9. (a) caned-ball valve; the first mechanical heart valve designed by Hufnagel in1952. (b) It was placed in the descending aorta. The ball simulates the leaflets of the valve. During the systole phase, the high blood pressure pushes the ball against the cage and opens the orifice

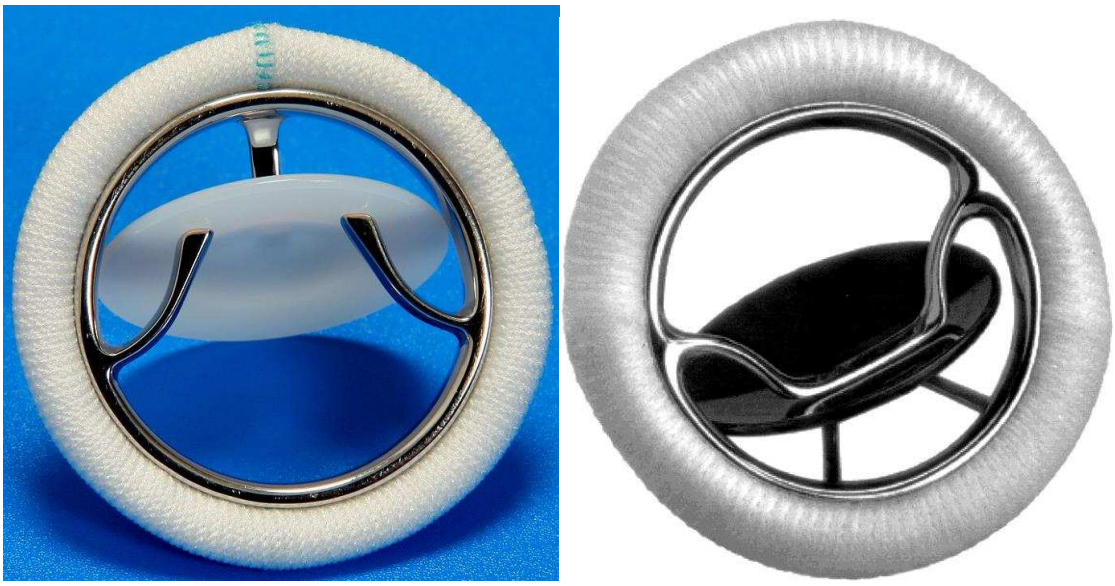

Figure 2.10. (a) Tilting- disc valve designed by Bjork-Shiley. (b) Tilting- disc valve designed by Lillehei-Kaster. The disc closes the valve orifice during diastolic pressure and tilt to side during the high blood pressure

Figure 2.11. Bileaflet heart valve designed by St Jude Medical Inc. It consists of two semicircular leaflets. Similar to previous cardiac valve designs the opening and closing mechanism of bileaflet heart valve is based on pressure gradient

Bioprosthetic heart valves are made of natural animal tissue which over chemical procedures became compatible with human body's internal environment. Figure 2.12 shows a sample of bioprosthetic valve which was designed by Carpentier-Edwards in 1991 (Mulholland, Lillemoe et al. 2012).

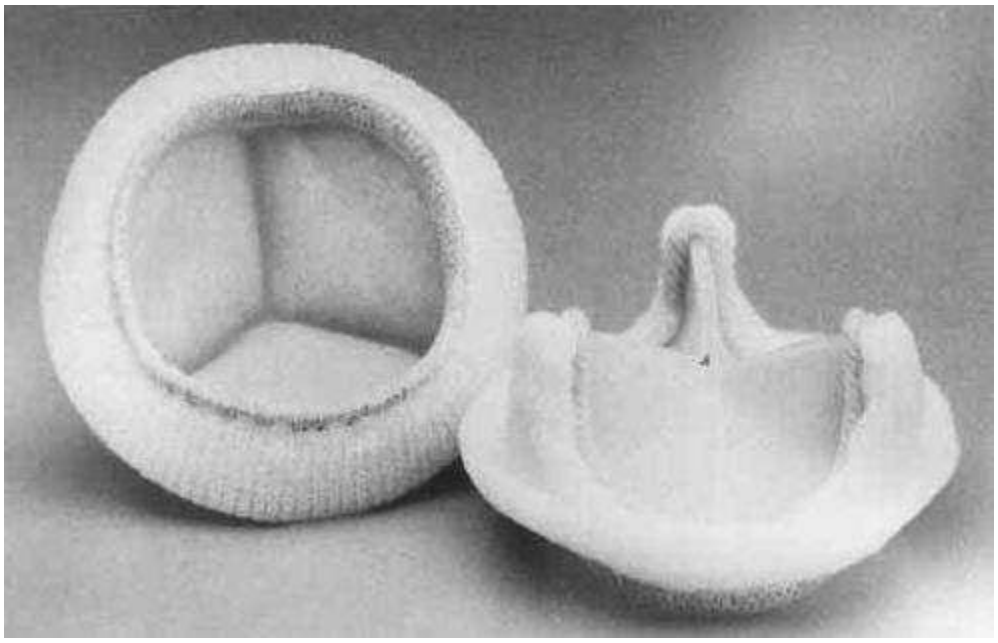

Figure 2.12. One of the firsts bioprosthetic valve designs by Carpentier-Edwards (Mulholland, Lillemoe et al. 2012)

Recently, transcatheter aortic valve implantation (TAVI) which is a less invasive heart valve replacement has been developed as an alternative for whom cannot take risk of open heart surgery. TAVI method inserts a stent valve at the location of valve through a catheter. In Figure 2.13, two types of TAV and their implantation procedure has been depicted.

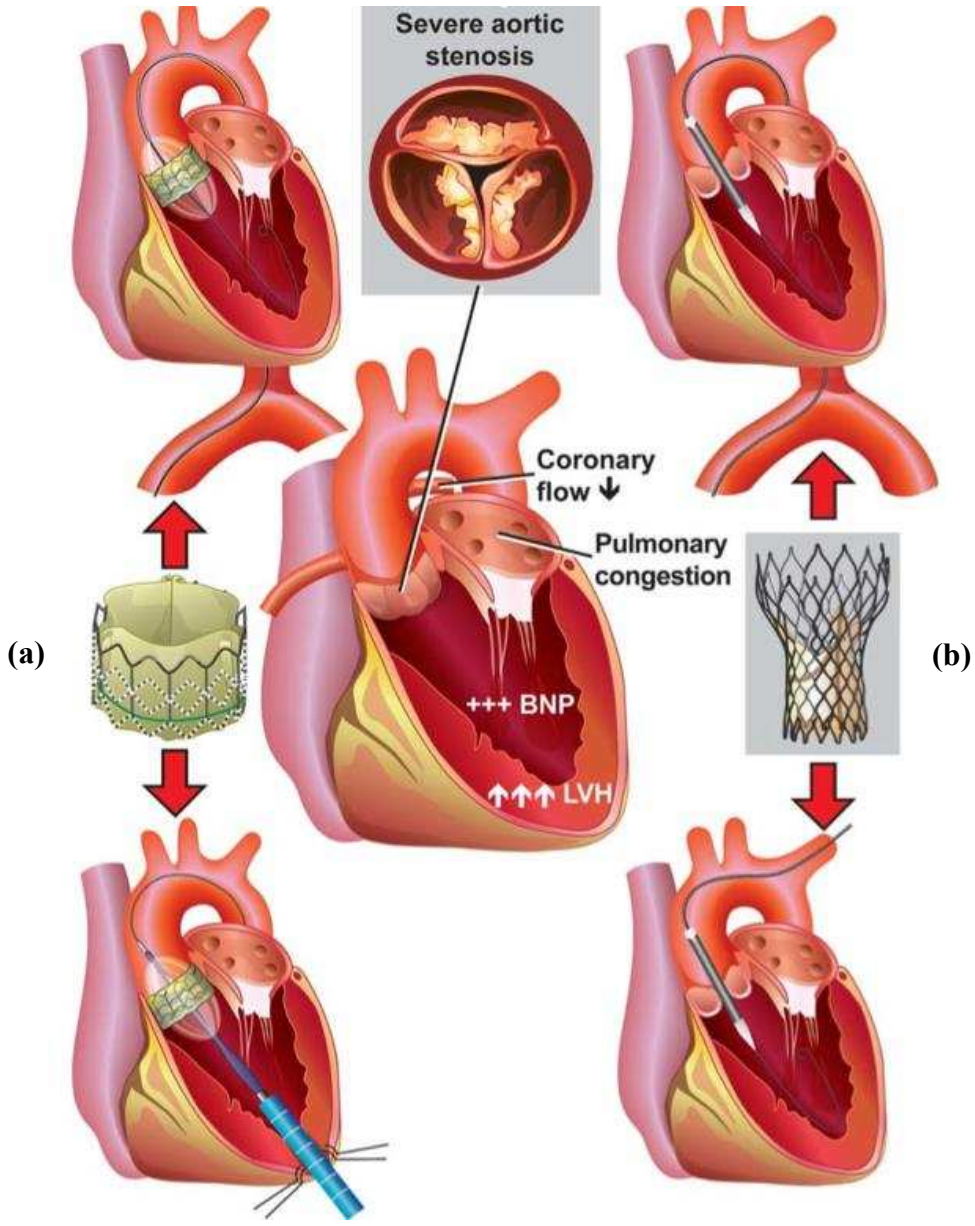

Figure 2.13. Transcatheter is used to deliver a balloon along with a stent valve into the location of aortic valve. Once TAV is placed, stenotic aortic valve start to function as a normal valve. Stent (a) is an Edwards SAPIEN THV valve (Edwards Lifesciences, Irvine, California) which is delivered from bottom of ventricle. Stent (b) is Medtronic CoreValve (Medtronic, Minneapolis, Minnesota) which is delivered from aortic side. Image is adapted from http://www.cardiachealth.org

3. AIM 1

The purpose of Aim 1 was to determine what biological and hemodynamic factors as well as anatomic parameters of native aortic valve are correlated with aortic valve calcification. In this Aim, calcification depositions in patient's CT scans were segmented using a 3D model reconstructing tool. The patient-specific geometric characteristics as well as hemodynamic and biological factors were extracted from patient's database and their relation with each cusp calcification was evaluated using multiple regression analysis.

3.1 Methods

3.1.1 Data Acquisition

A total of thirty patients including men and women were studied (age 80 ± 15 years, 57% men). All study protocols complied with the Institutional Review Boards of Medical Center of the Rockies (Loveland, CO, USA) and the Colorado State University. Patients referred to Medical Center of the Rockies for multislice computed tomography (MSCT) of the chest. The MSCT examinations were performed with a Philips Brilliance 64 channel CT scanner (Philips Healthcare, Amsterdam, Netherlands). In this data acquisition protocol, the thickness of slices was 0.67 mm, the vertical spacing between the pixels was 0.33 mm and horizontal pixel spacing was 0.748 mm. Constructed images were in DICOM format and grayscale color. The images were recorded in angiogram mode to evaluate coronary arteries. Data set has been studies before TAVI procedure. The population has been later treated by Edwards SAPIEN TAVIs and Medtronic CoreValves.

3.1.2 Medical Image Processing

3D models were constructed from CT scan images using ITK-SNAP version 3.2 (Yushkevich, Piven et al. 2006). In the 3D models, calcified lesions of RCC, NCC and LCC regions as well as RCA and LCA were segmented using a thresholding technique. Patient-specific aortic valve roots were extracted from whole body. The calcium volume in ITK-SNAP were measured in mm^3 on each of the RC, NC and LC sinuses and leaflets as well as the right and left coronary arteries (Figure 3.1).

(A)

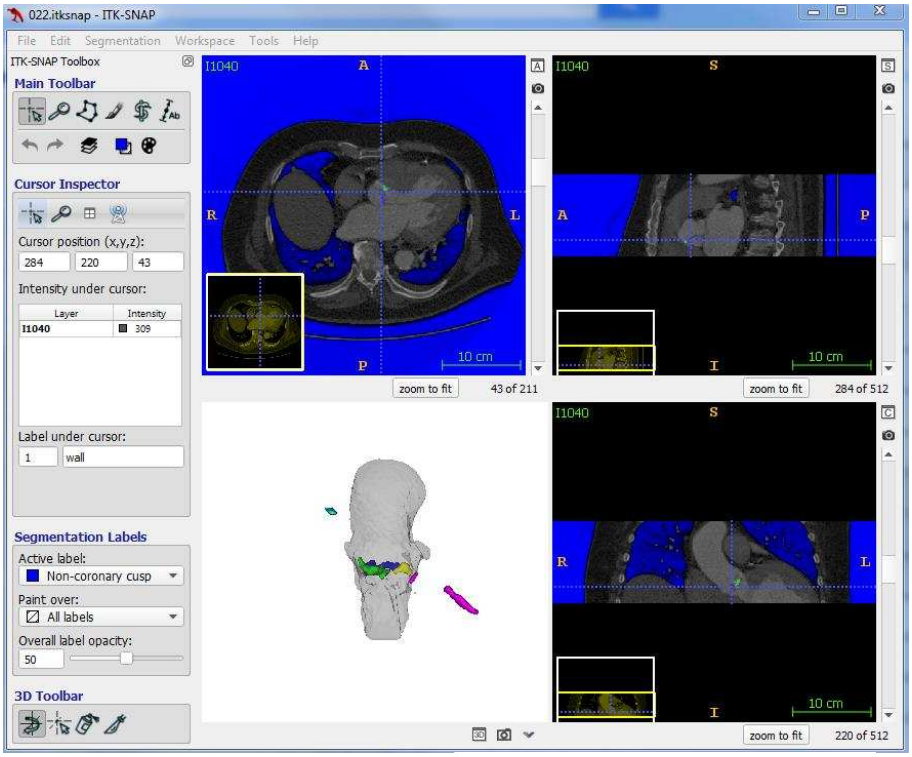

(B)

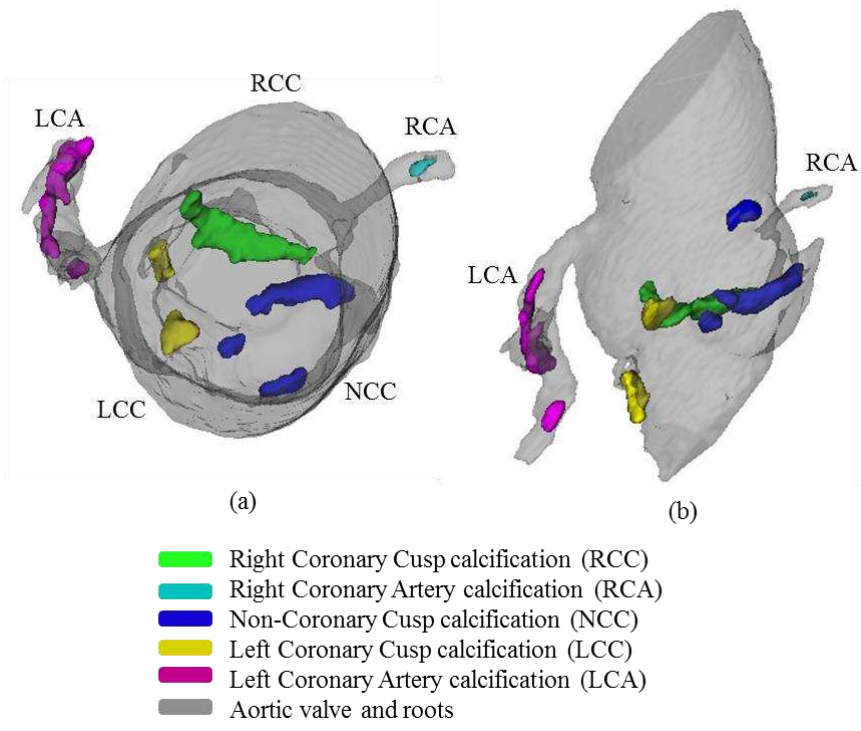

Figure 3.1. Screenshot of 3D model created in ITK-SNAP. (A) Thresholding was used to segment white (calcium) from grey areas. (B) Calcified lesions are represented in 5 colors in axial (a) and sagittal views (b)

3.1.3 Feature Extraction

Anatomical properties such as sinus of valsava (SoV) diameter, annulus diameter, sinotubular junction (STJ) diameter and coronary ostium distances from annulus wall were measured from 2D CT images by specialists at MCR and also using RadiAnt DICOM Viewer version 1.9.16 (Meixant, Poznan, Poland) (see Figure 3.2). Coronary calcifications were segmented from CT scan images. Hemodynamic features including left ventricle ejection fraction (LVEF), aortic valve peak velocity, mean pressure gradient, peak stenotic pressure gradient, aortic insufficiency (regurgitation) and hypertension as well as albumin level, body mass index (BMI), smoking and diabetes reported by MCR were extracted from data set.

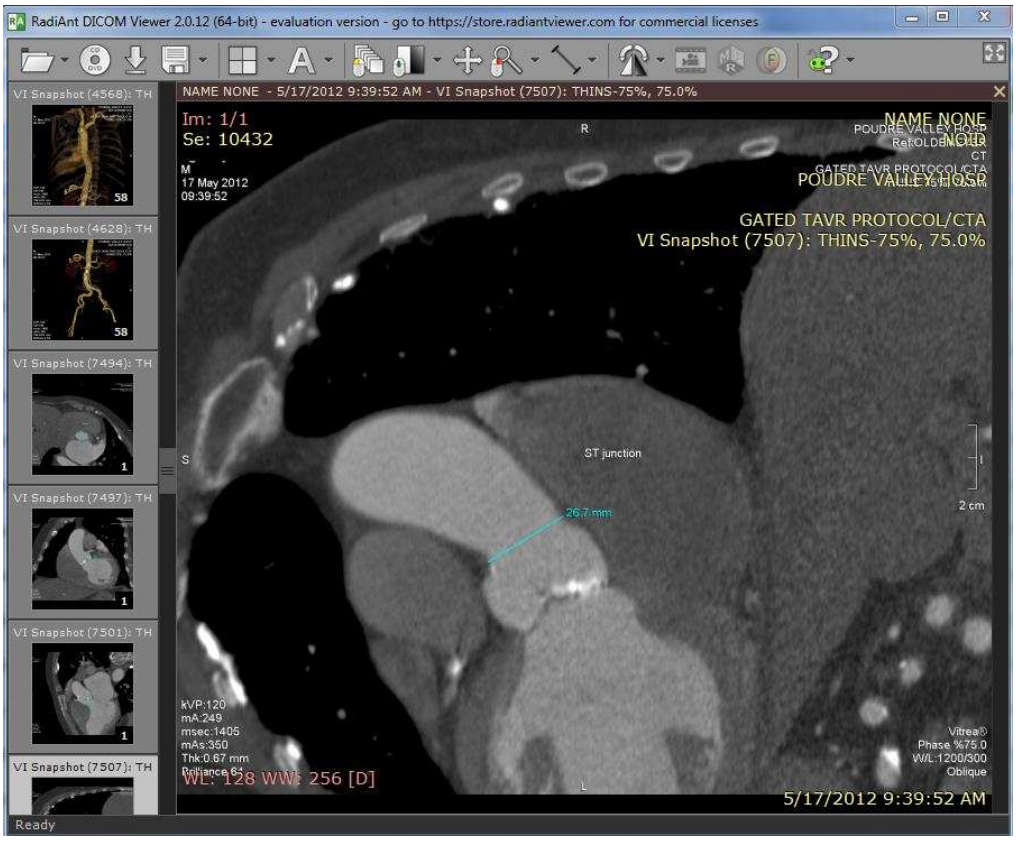

Figure 3. 2. Screenshot of the MicroDicom Viewer user interface. Measurement of STJ diameter

The factors have been selected based on previous studies. In several studies dimension of aortic valve cusps and aortic roots have been evaluated with multislice computed tomography and provided knowledge of relationship among STJ, annulus and coronary arteries (Tops, Wood et al. 2008; Schäfers, Schmied et al. 2013). Anatomical information of aortic valve helps to characterize calcification and avoid paravalvular leak or coronary calcification (Tops, Wood et al. 2008). Additionally, specific anatomical configuration in aortic valve and aortic roots leads to specific hemodynamic behavior in those regions. Hemodynamic and mechanical forces cause tissue deformation and inflammation (Balachandran, Sucosky et al. 2009). Moreover, low LVEF and BMI were considered to be related to high amount of calcification in the elderly people (Lindroos, Kupari et al. 1994; Zsuzsanna, Theodora et al. 2013). CRD is associated with low albumin level in blood. Albumin helps with fluid removal from tissue. Schiffrin suggested that albumin is an independent risk factor for cardiovascular calcification disease (Schiffrin, Lipman et al. 2007).

3.1.4 Statistical Analysis

Measured total calcium volume of RCC, NCC and LCC areas for 30 patients were between 40 mm^3 and 1800 mm^3. Severity of calcification can be classified into minimal (<25%), mild (25% < <50%), moderate (50% < < 75%) and severe (>75%) categories (Rivard, Bartel et al. 2009). In our dataset, only a few patients were placed in moderate and severe groups. Therefore in order to perform proper statistical analysis, patients with moderate and severe calcification were assigned into severe group. ANOVA pairwise comparison was performed for 30 patients (57% men) in order to compare differences of average calcification volume of RCC, NCC and LCC among men versus women as well as people with coronary calcification versus people without coronary calcification. For 95% confidence interval variables with p-value <0.05 were

considered significantly different. Multivariable linear regression method was used to estimate a relationship between variables and severity of calcification. For 4 patients, some information was not reported in the data set. Thus, those patients have been eliminated from multivariable regression test. The calcification distribution in three aortic valve cusps with respect to three categories of minimal, mild and severe has been evaluated. All analyses were performed using SAS university edition (SAS institute Inc., Cary, NC, USA).

3.2 Results

3.2.1 Baseline Characterization

Calcium in RCC, NCC and LCC of men and women was widely distributed. The average ± standard deviation for each feature is shown in Table 3.1 for men and women. Table 3.2 demonstrates the average ± standard deviation for all patients within groups of minimal, mild and severe calcification.

Table 3. 1. Baseline characteristics between men and women

Features	Men (13)	Women (13)	Total (26)	P-value
Calcium volume (mm^3): RCC NCC LCC	186±134 266±214 255±257	58±82 112±141 94±121	134±133 205±203 191±225	0.007* 0.028* 0.012*
RCA calcification (mm^3)	27±32	15±31	22±32	0.714
LCA calcification (mm^3)	262+207	50±60	170±192	0.007*
Age (years)	82±8	84±6	83±7	0.436
Height (cm)	169.5±8	160.5±13.5	165±12	0.057
Weight (kg)	73±16	72±15	72±16	0.867
BMI (kg/m^2)	0.43±0.1	0.45±0.09	0.44±0.09	0.646
LVEF	51±13	61±12	56±13	0.062
Hypertension	85% (11)	100% (13)	92% (24)	N/A
AV mean Pressure gradient (mmHg)	43±8	47±12	45±10	0.353
Annulus diameter (mm)	25±2	22±2.5	23±3	0.002*
STJ diameter (mm)	27±2	24±2.5	26±2.7	0.002*
SoV diameter (mm)	34±3	31±3	33±3	0.044*
Smoking	15% (2)	0	7.70%	N/A
Diabetes	15% (2)	15% (2)	15% (4)	N/A
Aortic Regurgitation: Trival = 0 Mild = 1 Moderate = 2 Severe = 3	7 5 0 1	7 3 2 1	14 8 2 2	N/A
Aortic stenosis	13	13	26	N/A
AV stenosis pressure gradient (mmHg)	70±12	80±20	75±17	0.145
Albumin (mg/dL)	4.16±0.25	3.97±0.39	4.06±0.35	0.185
AV morphology	Tricuspid	Tricuspid	Tricuspid	N/A
AV peak velocity	4.05±0.4	4.55±0.5	4.30±0.52	0.011*

Coronary cusp (RCC), non-coronary cusp (NCC), left coronary cusp (LCC), body mass index (BMI), left ventricle ejection fraction (LVEF), sinotubular junction (STJ), sinus of Valsalva (SoV), aortic valve (AV)

Table 3. 2. Baseline characteristics among minimal, mild and severe groups

Features	Minimal (12)	Mild (7)	Severe (7)
Calcium volume (mm3) RCC NCC LCC	51±63 83±69 51±44	146±70 184±130 174±94	175±96 453±231 279±178
RCA calcification (mm^3)	7.8±11	4.3±5	47±45
LCA calcification (mm^3)	38±41	112±95	341±211
Age (years)	85±5	81±7	79±8
Height (cm)	160±14	170±8	168±7
Weight (kg)	69±11	70±20	80±16
BMI (kg/m^2)	0.4±0.07	0.4±0.1	0.5±0.1
LVEF	62±12	56±11	46±11
Hypertension	100% (12)	71% (5)	100% (7)
AV mean Pressure gradient (mmHg)	47±12	41±8	45±8
Annulus diameter (mm)	22.3±2.6	24.6±3	24.6±2
STJ diameter (mm)	25±2.6	26±3	27±1.5
SoV diameter (mm)	31±2	31±3	36±1.5
Smoking	0	0	28% (2)
Diabetes	17% (20)	0	28% (2)
Aortic Regurgitation Trival = 0 Mild = 1 Moderate = 2 Severe = 3	7 3 1 1	4 3 0 0	3 2 1 1
Aortic stenosis	12	7	7
AV stenosis pressure gradient	81±20	68±12	70±10
Albumin	4±0.4	4.1±0.3	4.2±0.1
AV morphology	Tricuspid	Tricuspid	Tricuspid
AV peak velocity	4.6±0.5	4±0.5	4.1±0.3

Coronary cusp (RCC), non-coronary cusp (NCC), left coronary cusp (LCC), body mass index (BMI), left ventricle ejection fraction (LVEF), sinotubular junction (STJ), sinus of Valsalva (SoV), aortic valve (AV)

3.2.2 Comparison Tests

In general, the average of NCC calcification was 39 % of the total aortic valve calcification and the average of LCC and RCC calcification were respectively 36% and 25% of the total calcification among all patients. The calcification volume for RCC, NCC and LCC is presented in Table 3.3. The average calcification of aortic valve in men was 2.7 times more than that in women (see Table 3.3). The average calcification of NCC was 14% higher than average calcification of RCC and 3% higher than that of LCC while, the average calcification of LCC was approximately 11% higher than the average calcification of RCC. Aortic valve was also evaluated among groups of minimal, mild and severe calcification (Figure 3.3). NCC calcification was the highest volume within each group.

Table 3. 3. Comparison of average of calcification by aortic cusp

Sex	RCC (mm^3)	NCC (mm^3)	LCC (mm^3)
Men	186±134.3	266±214.6	255± 257
Women	58±82.4	112±141.1	94±121.9
Total	134±132.6	205±202.7	191±225.6

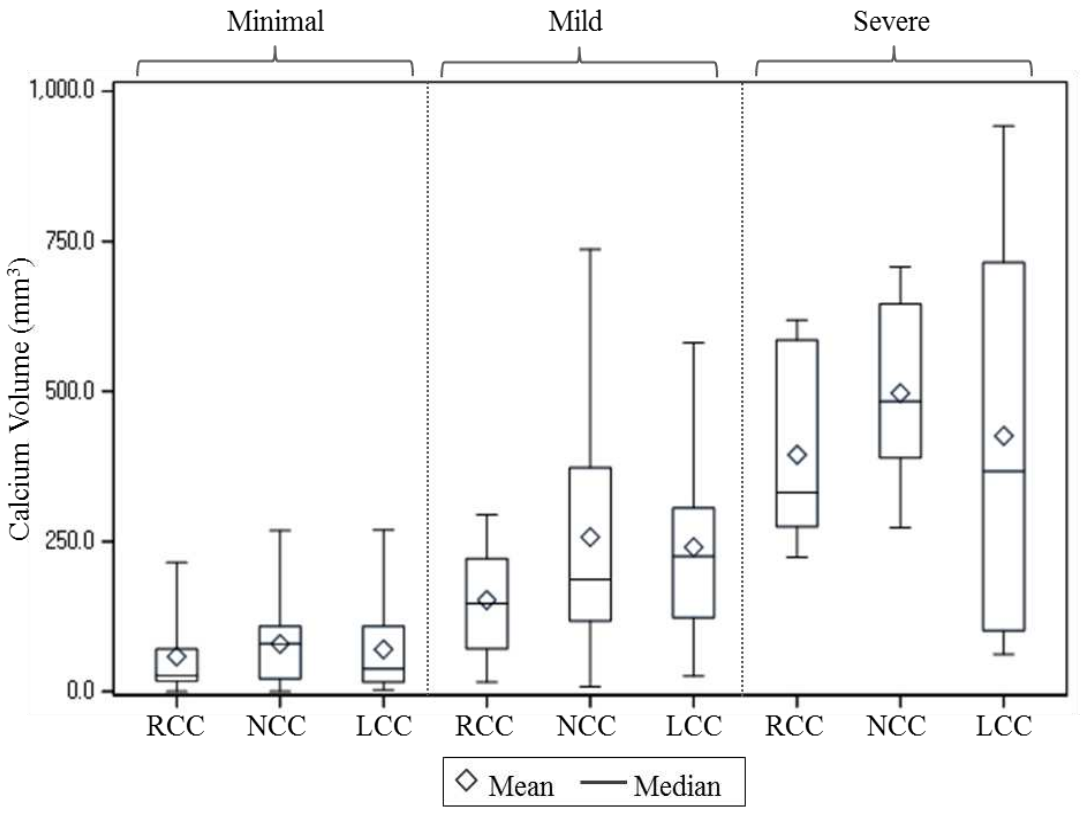

Figure 3. 3. The comparison of calcification distribution among three sinuses indicates that NCC is the most highly calcified cusp within each category

Table 3.4 indicates that in 57% (17 patients including 8 men and 9 women) of the cases, NCC was severely calcified. In 33% (10 patients including 7 men and 3 women) of the patients and in 10% (3 patients including 2 men and 1 women) LCC and RCC were respectively more calcified than others areas. Previous studies also confirmed that the first and the second highly calcified locations were respectively NCC and LCC while lower calcification volume was in RCC for both men and women (Halevi, Hamdan et al. 2015). Comparison between men and women showed that AVC in men was significantly higher than AVC in women (p-value = 0.002) (Figure 3.4). Results of AVC comparison between patients with low coronary artery calcification and high coronary calcification shows that in patients whom coronary arteries were highly calcified, the calcification in RCC (p-value=0.03), in NCC (p-value<0.001) and in LCC

(p-value<0.001) was significantly higher than those with low coronary calcification (Figure 3.5). Additionally, RCA calcification was significantly lower than LCA calcification in the studied population (p-value <0.001).

Table 3. 4. Location of AVC versus the severity of calcification

	RCC	NCC	LCC
Men			
Less calcification	13%	20%	23%
Medium calcification	37%	10%	10%
More calcification	6.6%	27%	23%
Women			
Less calcification	24%	10%	10%
Medium calcification	16.3%	3.3%	23%
More calcification	3.3%	30%	10%
Total			
Less calcification	37%	30%	33%
Medium calcification	53.3%	13.3%	33.3%
More calcification	10%	57%	33%

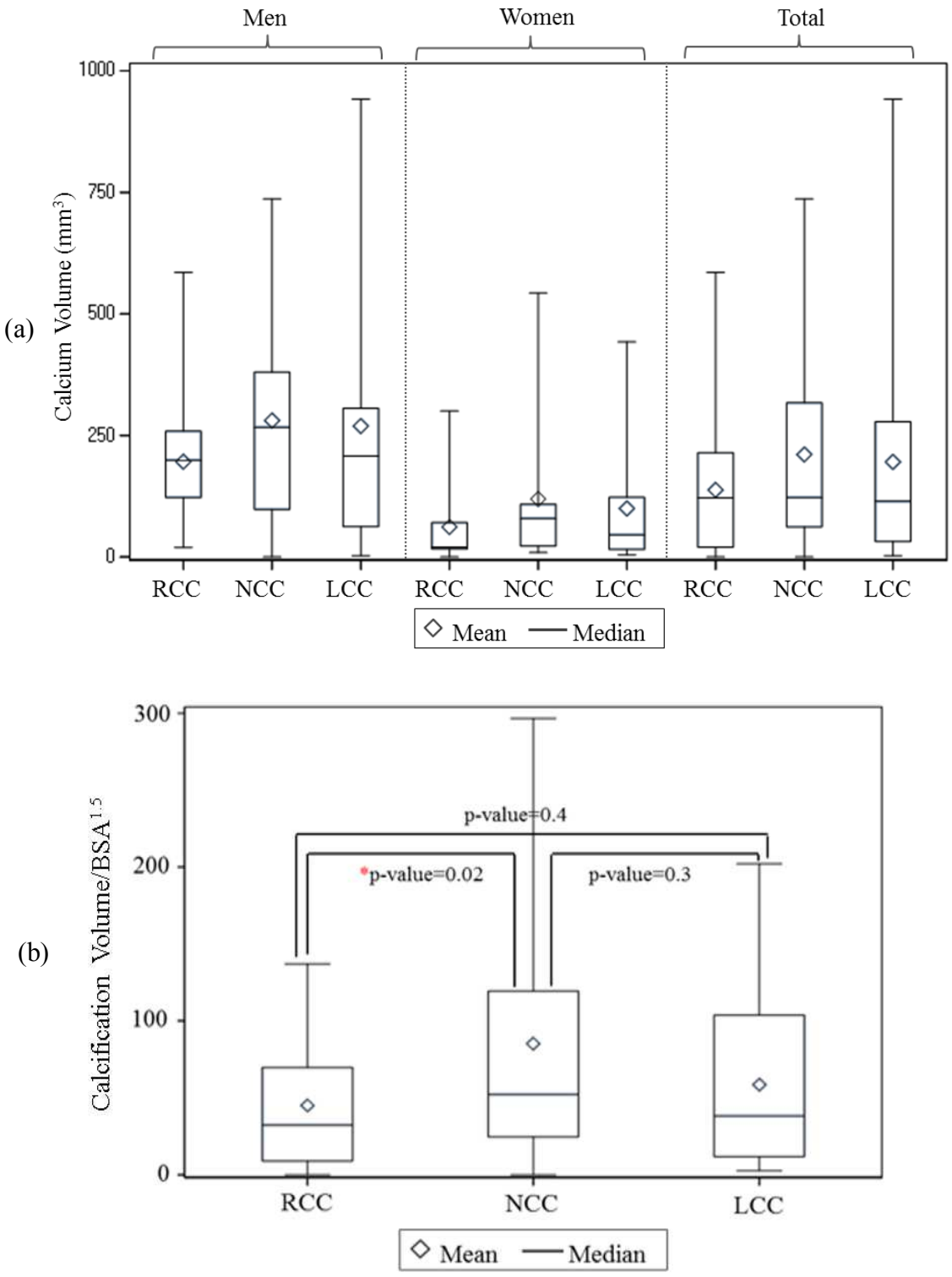

Figure 3. 4. (a) Distribution of calcification among right coronary cusp (RCC), non-coronary cusp (NCC) and left coronary cusp (LCC) between men and women. (b) The comparison of RCC, NCC and LCC areas indicate that the average normalized calcification volume on NCC is significantly higher than RCC, while there is no other significant differences among these 3 groups.

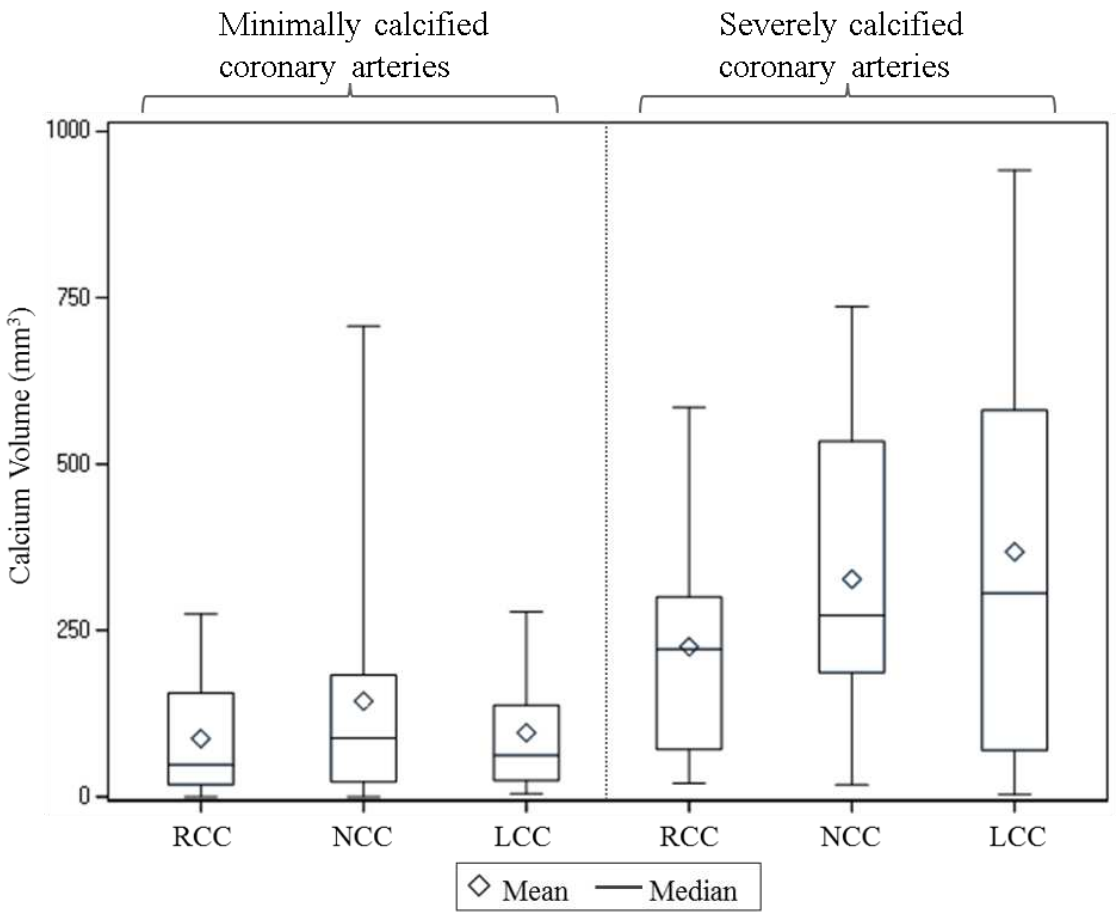

Figure 3. 5. Distribution of calcification by right coronary, non-coronary and left coronary cusps for patients with minimally calcified coronary arteries and patients with highly calcified coronary arteries. The comparison showed that patients with highly calcified coronary arteries had more AVC

3.2.3 Multivariable Regression Modeling

Multivariable regression analysis was performed to estimate the relationship between independent and dependent variables. In various studies, it has been suggested that extracted anatomic, hemodynamic and biological features separately play a role in calcification of aortic valve. Thus, we first performed regression analysis with the total calcification of aortic valve as dependent variable and all extracted features as independent variables. This model had R^2=0.92, however, it has been inferred that a model with too many variables always have a large R^2,

because existence of too many variables makes an overfitting model which models the random noise in the data. Therefore, we used feature selection method to avoid overfitting the model.

The three feature selection methods; forward, backward elimination and stepwise were used to ensure the reliability of the model. In the forward method, regression begins with no variable and sequentially adds significant variables to model. In the backward elimination, regression begins with considering all independent variables in the model and sequentially removes the non-significant variables from the model. Stepwise selection only applies statistically significant independent variables in regression model. In this study, the three feature selection methods had the same results. Significance level of 0.05 was considered to evaluate statistical differences of features. Separate models are presented for AVC based on coronary calcifications as well as anatomic characteristics of patients' native aortic valve. The following linear models with R^2 = 0.64 were obtained for men and women in equations (1) and (2):

(1) Men: (a) $Ca_{AV} = 75 \cdot D_{SOV} - 57 \cdot D_{STJ} - 340$

(b) $Ca_{AV} = 4.7 \cdot Ca_{RCA} + 0.46 \cdot Ca_{LCA} + 449$

(2) Women: (a) $Ca_{AV} = 75 \cdot D_{SOV} - 57 \cdot D_{STJ} - 692$

(b) $Ca_{AV} = 4.7 \cdot Ca_{RCA} + 0.46 \cdot Ca_{LCA} + 185$

Where Ca_{AV}, Ca_{RCA} and Ca_{LCA} are in mm^3, Ca_{AV} shows calcification volume in three aortic cusps (right, left and non-coronary) and Ca_{RCA} and Ca_{LCA} in part (b) of (1) and (2) equations indicate calcification in the right and left coronary arteries. The D_{SoV} and D_{STJ} are diameters of sinus of valsava and sinotubular junction, respectively. The SoV and STJ diameters are in mm.

Since calcification of aortic valve in men was significantly more than AVC in women, the estimated intercepts for women was smaller than the intercepts in men's equations. All four independent features were statistically significant (p-value << 0.05). The positive and negative coefficients indicate that the total calcification of aortic valve increases with increase in SoV diameter and decrease in STJ diameter. Although, the regression model showed a strong correlation between calcification in coronary arteries and calcification in three aortic cusps, this correlation is not causation. The other examined features such as AV peak velocity, pressure gradient, LVEF, hypertension and aortic insufficiency as well as albumin level, smoke and diabetes were not statistically significant in our population. Therefore, zero coefficients were assigned to them.

3.3 Discussion

Our results and multiple studies (Ewe, Ng et al. 2011; Koh, Lam et al. 2015) suggested that the NCC calcifies more than LCC and RCC areas. It has been hypothesized that absence of diastolic coronary flow in NCC causes low shear stress in this area which explains why non-coronary is often more calcified than other areas (Freeman and Otto 2005; Moore and Dasi 2015). In present study, calcification in LCA was significantly higher than RCA calcification. McCarthy investigation also showed that calcification formation is more common in LCA rather than RCA and coronary artery calcification is strongly associated with aortic valve calcification (McCarthy and Palmer 1974). This significant difference among calcification of LCA and RCA is perhaps due to anatomical structure of coronary ostiums. Several studies reported that right coronary ostium is naturally farther than left coronary ostium from aortic annulus which is important in development of disease (Knight, Kurtcuoglu et al. 2009; Rivard, Bartel et al. 2009). In present study, the length of right and left coronary ostiums from base of aortic annulus was respectively

17±4.8 and 14.3±5. Calcification in coronary arteries narrows the arterial area and leads to change in hemodynamics of aortic valve sinuses, therefore, flow rate decreases when passing through narrowed artery. This low coronary flow rate causes low magnitude vorticity which is associated with calcification (Moore 2015).

Results of our regression model showed that calcification of aortic valve is associated with calcification in right and left coronary arteries (RCA and LCA). In fact, correlation between coronary artery calcification and aortic valve calcification does not imply that one causes the other but perhaps there is another factor which simultaneously affects development of calcification process in both coronary artery and aortic valve. The prediction model represents that patients with large sinus of valsava (SoV) and small sinotubular junction (STJ) diameters are more susceptible to calcific aortic valve disease. In other words, aortic valve will be in a healthy condition if SoV diameter is relatively small while STJ diameter is relatively large. Previous investigations suggested that the large STJ diameter improves valvular hemodynamics (Dagum, Green et al. 1999) and the large SoV diameter deteriorate hemodynamics of aortic sinuses (Moore 2015). Marom et al. experiments also indicated that the ratio of STJ to annulus diameter significantly changes hemodynamics and flow shear stress in aortic cusps (Marom, Halevi et al. 2013). Thubrikar suggested that SoV is very important in minimizing stress in the valve leaflets (Beck, Thubrikar et al. 2001). Moore also supported this hypothesis with his hemodynamic experiments on sinus size; in a narrow sinus, sinus vortex practically does not exist and in a wide sinus, sinus vortex loses its strength and disappears gradually (Moore 2015) (Figure 3.6). Moore suggested that average sinus of valsava diameter yields ideal hemodynamic condition; therefore further investigation is needed to acquire an optimized ratio between SoV and STJ diameters with respect to annulus size for a healthy valve condition.

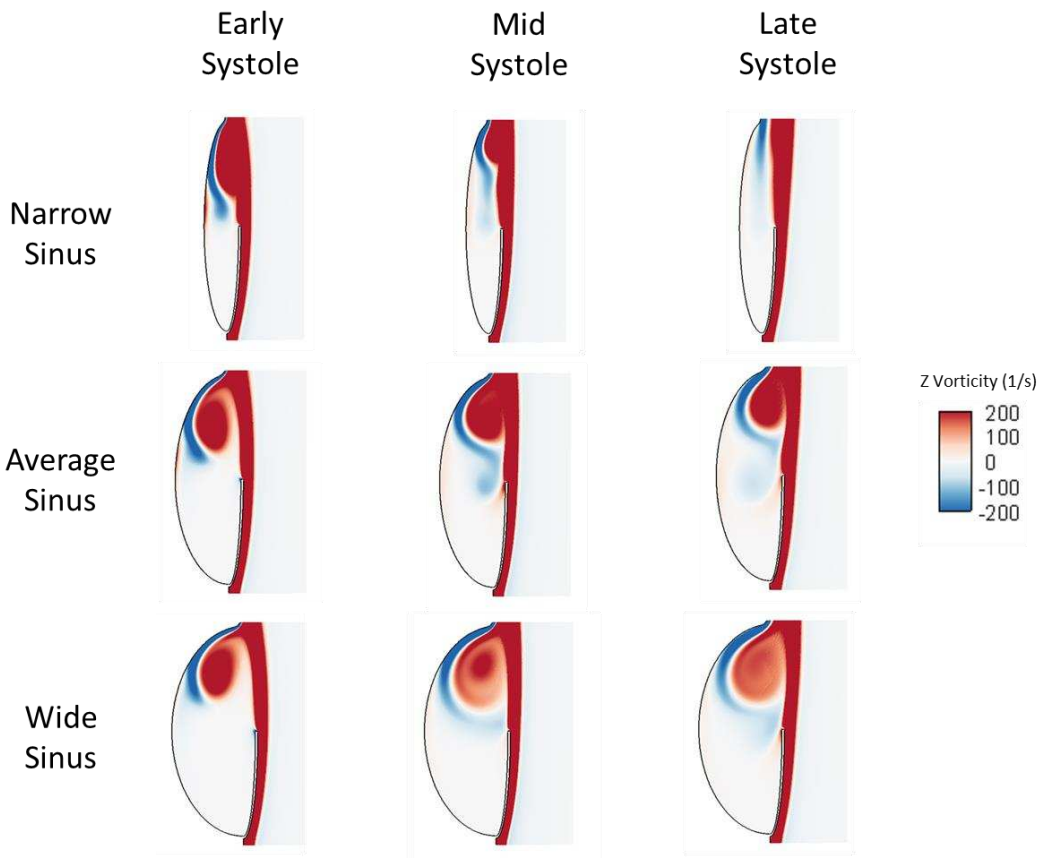

Figure 3.6. Three different 2D models represent different sinus radii and vorticity contours at three systolic time points. Hemodynamic condition in average sinus size is better than narrow and wide sinus sizes. The figure is adapted from Moore 2015.

In our data set, albumin level, BMI, stenotic pressure gradient, mean pressure gradient, peak velocity, hypertension and LVEF as well as diabetes and smoking were not significantly different in the regression model. To conclude, we introduce that sinotubular junction and sinus of valsava diameters of native aortic valve are primary predictors of aortic valve calcification. Aortic valve calcification disease is a multiscale process in which anatomical configuration of aortic valve shapes hemodynamics within the aortic sinuses, then hemodynamic forces will be transmitted to cells and tissue and cause cellular deformation and eventually leads to calcification.

4. AIM 2

The purpose of Aim 2 was to determine the relationship among patients' calcification level and anatomic parameters of their native aortic valve as well as the risk of post-procedural PVL occurrence. In this Aim, patient-specific calcification which was segmented in Aim 1, was compare with TEE of patients to find the exact location of post-procedural PVL. Relationship of post-procedural PVL with anatomic parameters and calcification level was evaluated by multiple logistic regression.

4.1 Methods

4.1.1 Data Acquisition

A total of thirty three patients with severe aortic stenosis who underwent TAVI were studied (age 80 ± 15 years, 48% men). All study protocols complied with the Institutional Review Boards of Medical Center of the Rockies (Loveland, CO, USA) and the Colorado State University. Patients were referred to Medical Center of the Rockies for multislice computed tomography (MSCT) of the chest. The MSCT examinations were performed with a Philips Brilliance 64 channel CT scanner (Philips Healthcare, Andover, MA, USA). In this data acquisition protocol, the thickness of slices was 0.67 mm, the vertical spacing between the pixels was 0.33 mm and horizontal pixel spacing was 0.748 mm. The images were recorded in angiogram mode to evaluate coronary arteries. Transesophageal echocardiography (TEE) was performed on the patients in order to assess valve function before and after TAVI procedure. The patients have been treated by thirty one Edwards SAPIEN TAVIs and two Medtronic CoreValves.

4.1.2 Transesophageal Echocardiography Assessment

Transesophageal echocardiography (TEE) has been frequently used to assess impact of aortic annulus dimension on occurrence of post-procedural aortic regurgitation (Santos, De Agustín et al. 2012). After implantation, short and long axis views of patient aortic valve were recorded using Philips iE33 xMATRIX echo system (Philips Healthcare, Andover, MA, USA). The presence of PVL was assessed by color Doppler flow imaging around the implanted stent. In the studied population, only mild and moderate PVL appeared after TAVI. To determine the exact location of PVL, 2D axis views (30° to 60°) were matched and compared to segmented 3D models of aortic valve using RadiAnt DICOM Viewer version 1.9.16 (Meixant, Poznan, Poland). Figure 4.1 is an example which demonstrates how TEEs of short and long axes were matched with 3D models of aortic root and calcification nodules to evaluate the location of PVL.

4.1.3 Medical Image Processing

3D models were constructed from CT scan images using ITK-SNAP version 3.2 (Yushkevich, Piven et al. 2006). In the 3D models, calcified lesions of RCC, NCC and LCC regions as well as RCA and LCA were segmented using a thresholding technique. Patient-specific aortic valve roots were extracted from whole body. The calcium volume in ITK-SNAP were measured in mm^3 on each of the RC, NC and LC cusps and leaflets as well as the right and left coronary arteries.

4.1.4 Feature Extraction

Anatomical properties such as sinus of valsava (SoV), aortic annulus (AA) and sinotubular junction (STJ) were measured from 2D CT images by Medical Center of the Rockies. Coronary calcifications were also segmented from CT scan images to be evaluated in relation to PVL.

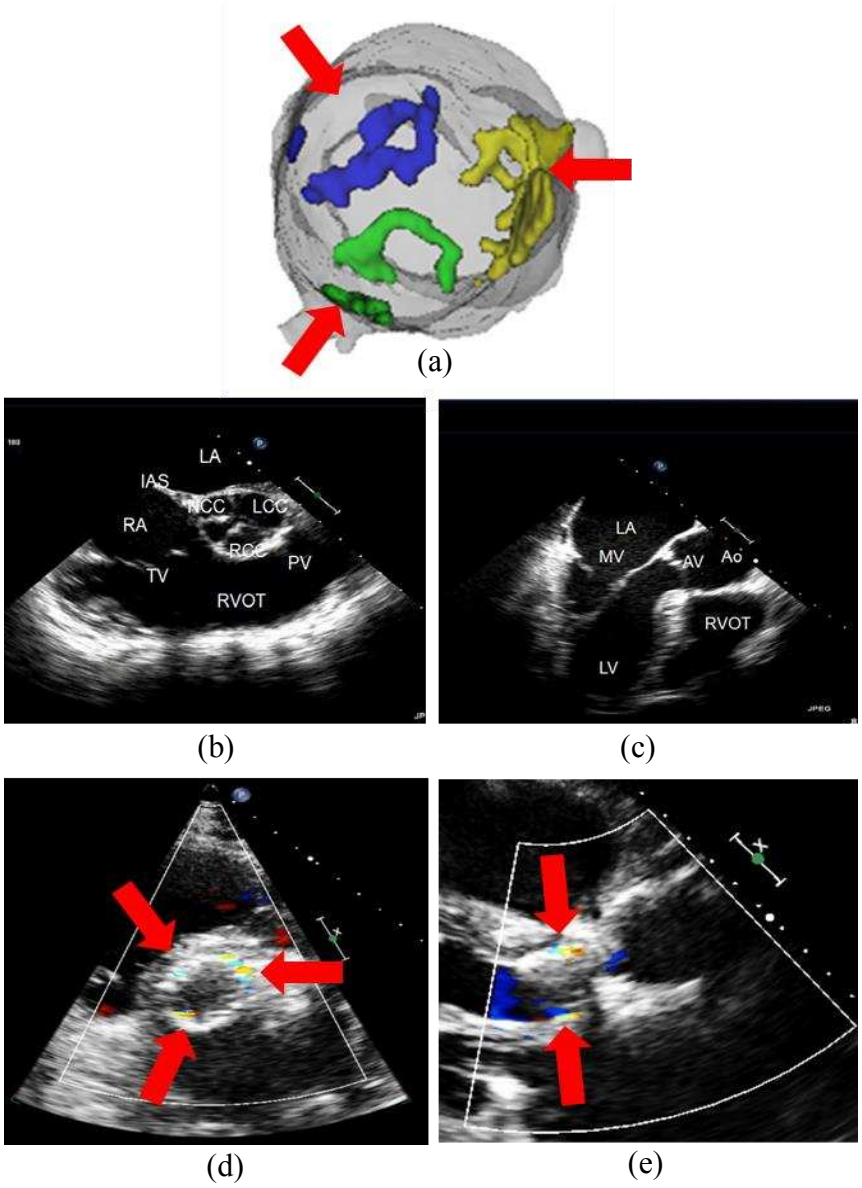

Figure 4.1. Example of matching (a) 3D model of calcification with 2D views of short (b, d) and long axes (c, e). Calcification in RCC, NCC and LCC is demonstrated with green, blue and yellow colors, respectively. Red arrows show the location of PVL

4.1.5 Statistical analysis

Multivariable linear regression method was performed to estimate a relationship for paravalvular leak based on anatomic variables and degree of calcification. Comparison tests were performed to show the significant differences among variables. For 95% confidence interval, variables with p-value <0.05 were considered statistically significant. P-values were calculated by Wilcoxon and T-tests based on the normality of data. All analyses were performed using SAS university edition (SAS institute Inc., Cary, NC, USA).

4.2 Results

4.2.1 Transesophageal Echocardiography Results

Location of aortic valve as well as aortic cusps and leaflets were determined in 2DTEE images. Aortic valve calcification in 2D TEE echoes was matched with AVC in the segmented 3D models and precise location of paravalvular leak in each patient was observed. In two patients out of 12, the exact location of PVL was not clear, therefore observational results of them are not reported. Observations indicated that 30 regions in the aortic valve of 10 patients underwent PVL. In the majority of patients who were diagnosed with both mild and moderate PVL, PVL has been observed from three regions. Among the ten patients who had post-procedural PVL (Figure 4.2), five PVL sites were observed at the location of RCC, four PVL sites were observed at commissure between right and non-coronary cusps, four PVL sites were observed at the location of NCC, four PVL sites were observed at commissure of non-coronary and left coronary cusps, six PVL sites were observed at the location LCC and seven PVL sites were observed at commissure between left coronary and right coronary cusps. PVL was observed from either

location of calcification in a cusp or commissure between two calcified cusps or even commissure between two cusps which were not severely calcified.

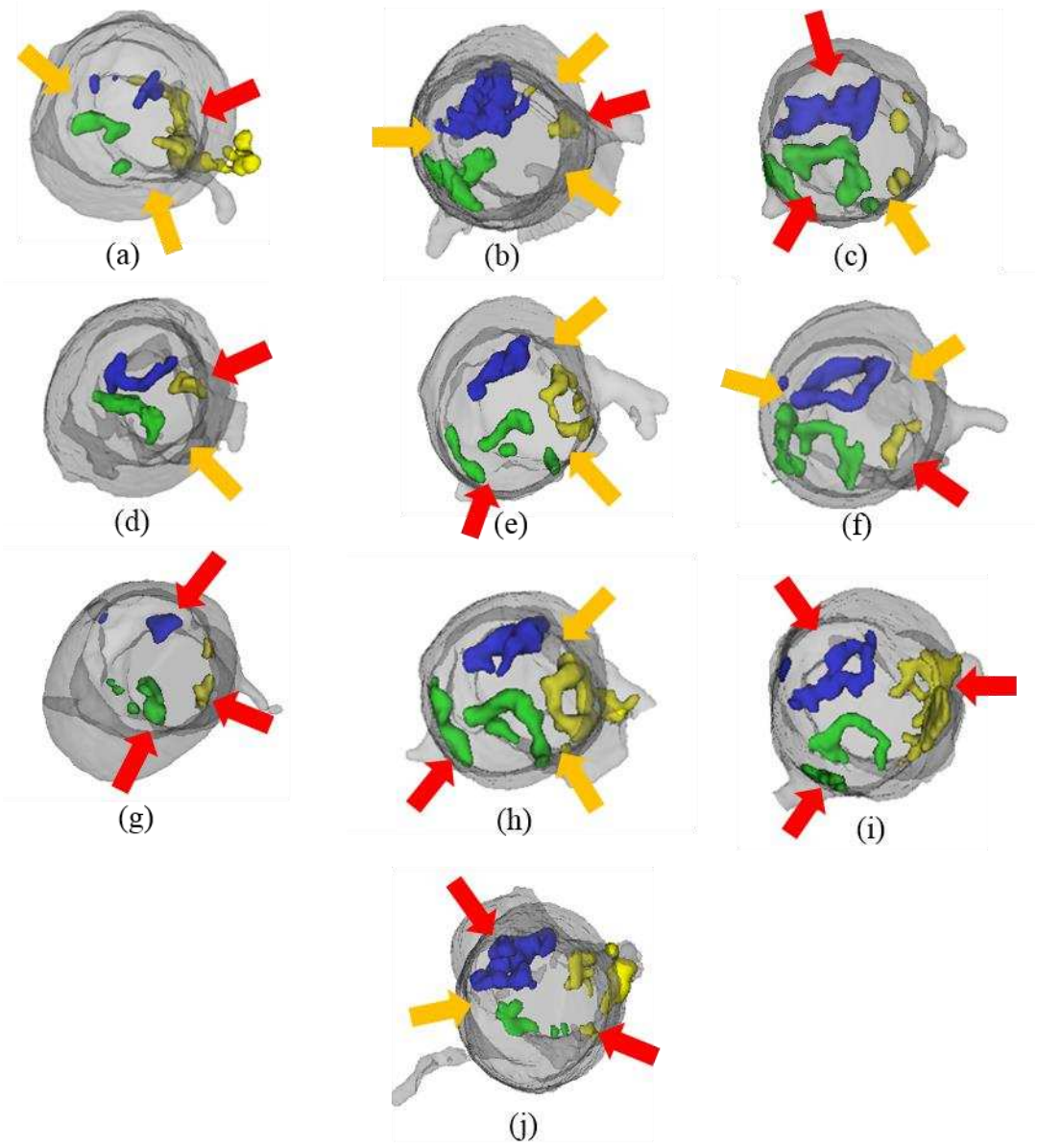

Figure 4.2. Calcification in RCC, NCC and LCC are presented with green, blue and yellow colors, respectively. Red arrows indicate that PVL occurs at cusp side while orange arrows indicate that PVL occurs at commissure between two cusps. PVL was observed from either location of calcification in a cusp or commissure between two calcified cusps or even commissure between two cusps which are not severely calcified. Figures (a) to (j) are sorted in the order of increasing aspect ratio of SoV/AA diameter

4.2.2 Comparison Tests

Baseline characterization of calcification and anatomical properties of patients is shown in Table 4.1. The measured total calcium volume for all patients was in range of 120 mm^3 to 1900 mm^3. The average aortic valve calcification within patients with PVL was about 3 times higher than that in patients without PVL (p-value<0.001) (Figure 4.3).

Table 4.1. Baseline characteristics

*Statistically significant

Abbreviations: Right coronary cusp (RCC), non-coronary cusp (NCC), left coronary cusp (LCC), right coronary artery (RCA), left coronary artery (LCA), aortic annulus (AA), sinotobular junction (STJ), sinus of valsava (SoV)

Variables	All (n=33)	Without Paravalvular Leak (n=21)	With Paravalvular Leak (n=12)	P-value
Men	48% (16)	48% (10)	50% (6)	N/A
Calcification Volume (mm^3):				
RCC	177 (0-830)	99 (0-260)	297 (70-830)	<0.001*
NCC	278(0-970)	152 (0-550)	471 (44-970)	0.001*
LCC	235 (10-930)	145 (10-580)	373 (74-930)	0.009*
Total	690 (120-1900)	397 (120-800)	1140 (400-1900)	<0.001*
RCA calcification	32 (0-340)	8 (0-50)	69 (0-340)	0.072
LCA calcification	157 (0-880)	107 (0-400)	234 (10-880)	0.071
AA diameter	23 (18-28)	23 (18-28)	22 (18-28)	0.245
STJ diameter	26 (20-34)	26 (20-34)	26 (21-34)	0.689
SoV diameter	33 (25-40)	32 (26-37)	33.5 (25-40)	0.561

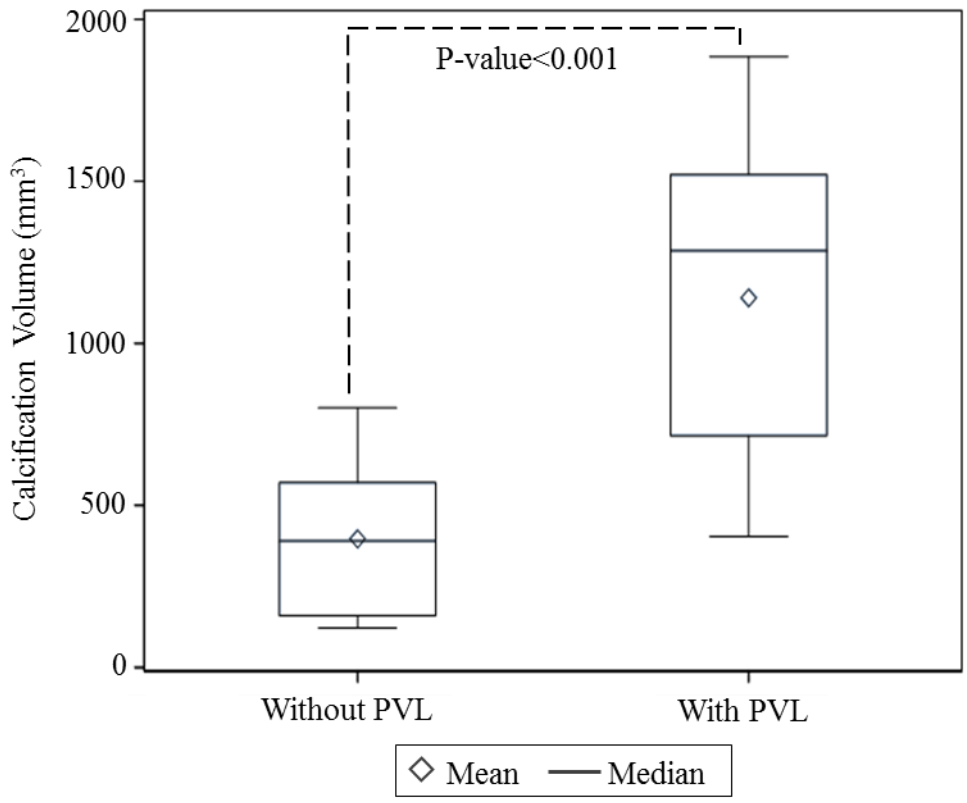

Figure 4.3. Comparison of AVC between patients with and patients without PVL shows that patients with PVL had significantly higher amount of AVC rather than patients without PVL.

Calcium deposition in each of the RCC, NCC and LCC in people with PVL was significantly higher than calcification at similar cusp in patients without PVL. Moreover, in both groups of patients with and without PVL that are shown in Table 4.1, NCC was more calcified than other cusps. In the studied population, comparison of calcification between groups of men and women showed that men's aortic valve calcification was about twice more than women's (p-value=0.003). Although anatomic parameters of annulus, STJ and SoV were not statistically significant within groups of with and without PVL, the aspect ratio of SoV/AA diameter was significantly higher in patients with PVL rather than patients without PVL (p-value=0.027) (Figure 4.4). Analysis of aortic valve calcification location in compared to paravalvular leak showed that in cases in which mild or moderate paravalvular leak has occurred, the average aortic valve calcification was approximately three times higher than average AVC in cases that

no paravalvular leak occurred (Table 4.2 and Figure 4.5), while AVC volume was not significantly different between mild and moderate PVL cases.

Table 4.2. Severity of paravalvular leak versus aortic valve calcification

Paravalvular leak	None	Mild	Moderate
Average calcification volume (mm^3)	396.8 (120-800)	1190 (400-1900)	1100 (420-1870)

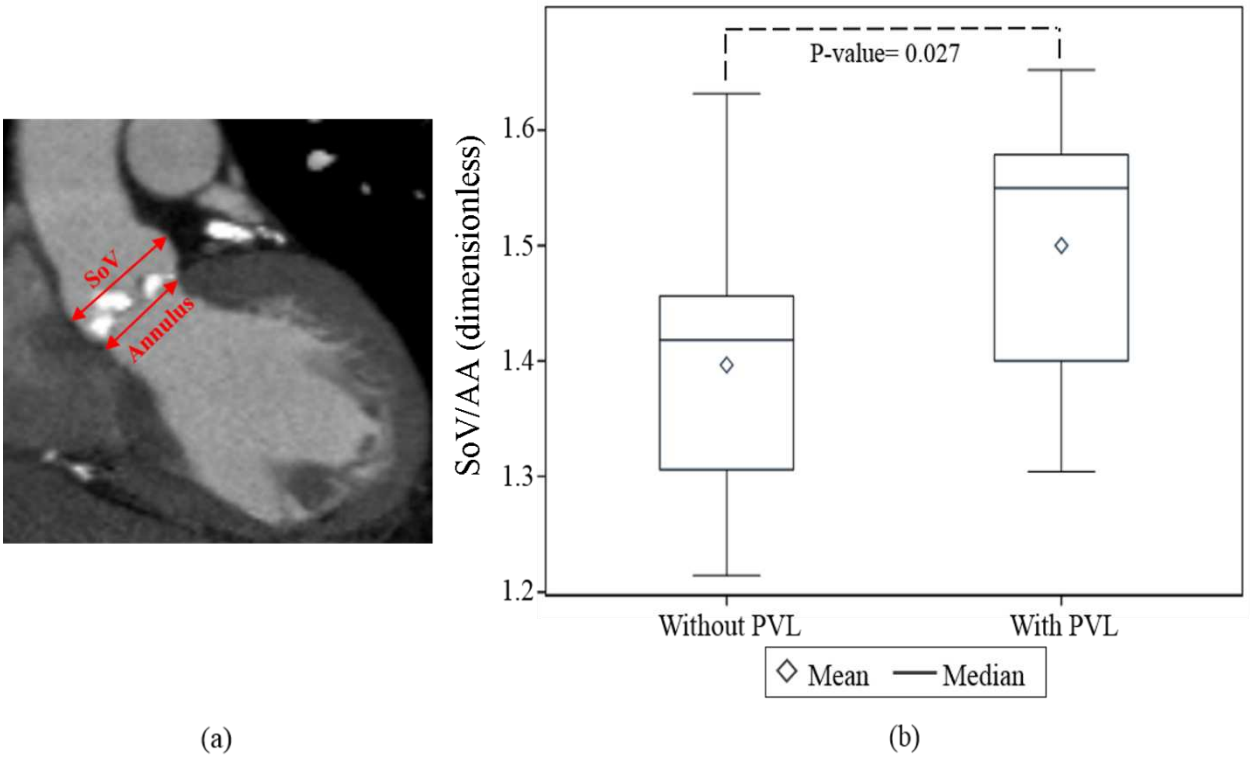

Figure 4.4. (a) Demonstration of the sinus of valsava (SoV) and annulus diameters of aortic valve. (b) Comparison of aspect ratio of SoV/AA between patients with and patients without PVL shows that patients with PVL had significantly bigger ratio of SoV/AA rather than patients without PVL.

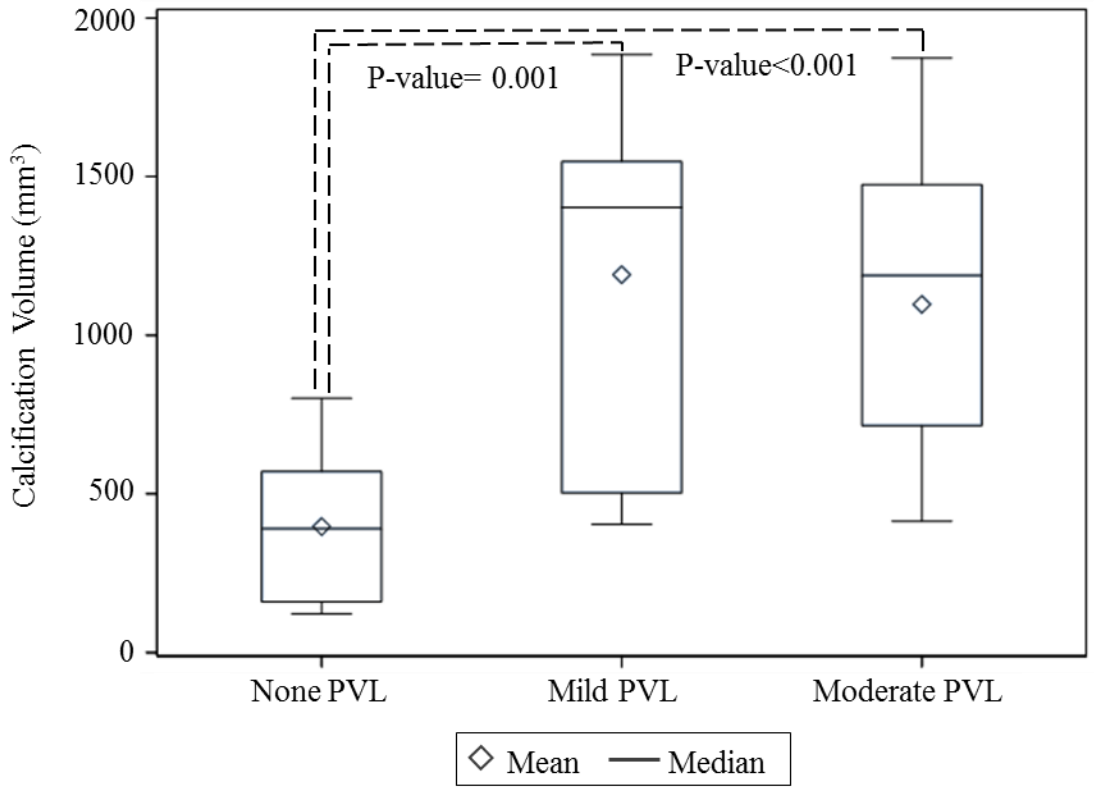

Figure 4.5. Comparison of AVC among groups with different severity of PVL shows that AVC in mild and moderate PVL groups was significantly higher than AVC in patients without PVL; while AVC between patient with mild and moderate PVL was not significantly different (p-value=0.75).

4.2.3 Multivariable Logistic Regression Modeling

Multivariable logistic regression analysis was performed to estimate a relationship for anatomic variables and aortic valve calcification with post-procedural paravalvular leak. In this analysis, AVC and anatomic parameters of native aortic valve including SoV, STJ and annulus diameters as well as various combination of ratio of these anatomic parameters, were evaluated. In this regression modeling, backward elimination method was used to find parameters that best fit the response variable (occurrence of PVL). In this method, regression begins with considering all independent variables in the model and sequentially removes the non-significant variables from the model. Significance level of 0.1 was considered to evaluate statistical differences of regression parameters. Regression model suggested that AVC and aspect ratio of SoV/AA as

well as men gender are highly correlated to post-procedural PVL. Therefore, these parameters are statistically significant (p-value<0.1) and are independent predictors for post-procedural PVL. The increase in both AVC and aspect ratio of SoV/AA increases the probability of PVL occurrence. The effect of predictors on probability of PVL occurrence is evaluated individually and combined. The probability graphs of PVL incident based on AVC and SoV/AA predictors as well as interaction of these parameters are presented in Figure 4.6. For example, the values of AVC, SoV/AA and interaction of parameters for a 50% occurrence probability of PVL are about 750 mm^3, 1.5 and 1100 mm^3, respectively. Since both AVC and SoV/AA parameters increases the risk of PVL occurrence, the interaction of them is also highly correlated to post-procedural PVL. Probability curve of interaction gives a better understanding to occurrence of PVL based on various combination of AVC and the ratio of SoV/AA. Since, men sex parameter is a categorical variable, no probability graph or ROC analysis is reported for this parameter.

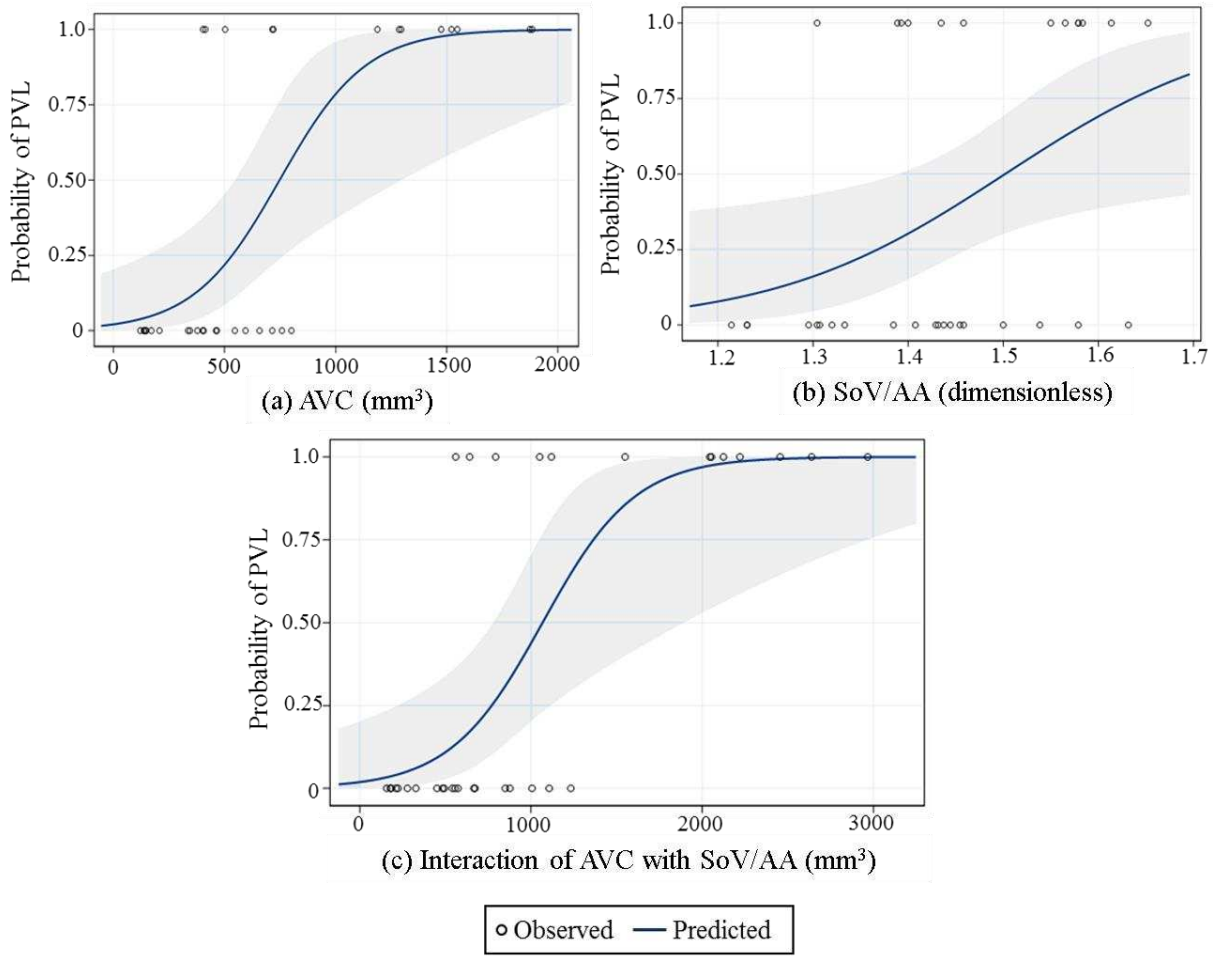

Figure 4.6. Probability of occurrence of post-procedural PVL with respect to (a) AVC (b) SoV/AA and (c) interaction of these two parameters. Probability of PVL occurrence can be estimated at each parameter value. The highlight area shows the confidence interval of the blue curve

4.2.4 Receiver Operator Characteristic Analysis

In order to evaluate the performance of predictor parameters in discriminating between patients with and without PVL, a receiver operator characteristic (ROC) analysis was performed for each predictor parameters as well as the possible interaction between two predictors. The possible interaction was assumed to be the product of AVC and aspect ratio of SoV/AA). ROC curve identifies the discriminating threshold level for each variable. The values of 1200 mm^3, 1.5 and 1330 mm^3 for AVC and aspect ratio of SoV/AA as well as interaction of these two parameters

are determined as threshold levels for discriminating between patients who may undergo PVL after TAVI procedure and patients who might remain safe against PVL. Patients with parameters below the threshold levels are expected to be safe against PVL while patients with parameters above the threshold levels are expected to undergo post-procedural PVL. However, at each threshold level (cutoff point), there might be errors (false positive and false negative) in discrimination between patients with and without post-procedural PVL. These errors are determined by ROC analysis. ROC curve is created by plotting the sensitivity versus 1-specificity for each predictor variable. Sensitivity or true positive rate indicates the correctly detection of patients who will experience post-procedural PVL. Specificity or true negative rate indicates the correctly detection of patients who will not experience post-procedural PVL. Thus, ROC curve helps to determine false positive and false negative errors at each cutoff value. The accuracy of the predictors in detection of PVL is shown by area under the ROC curve of each parameter. The area under the ROC curve for AVC, aspect ratio of SoV/AA and interaction of parameters are 0.89 (95% CI= 0.78-1.0), 0.73 (95% CI= 0.55-0.91) and 0.91 (95% CI= 0.81-1.0), respectively (Figure 4.7). At the mentioned optimum cutoff values (threshold levels), the sensitivity and specificity were maximized while false positives and false negatives were minimized (Table 4.3).

Table 4.3. ROC analysis at cutoff points (optimum threshold value)

Variable	Sensitivity	Specificity	False positive	False negative
AVC	62%	100%	0%	20%
SoV/AA	53%	85%	30%	26%
AVC × SoV/AA	62%	100%	0%	20%

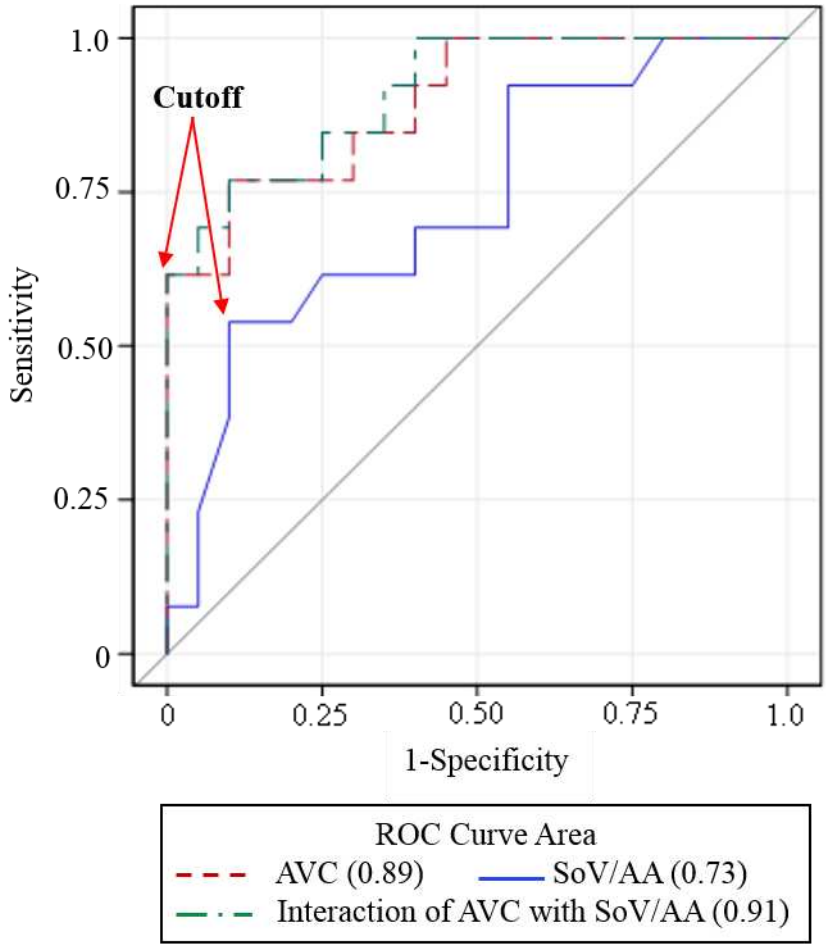

Figure 4.7. Accuracy of each predictor in discriminating post-procedural PVL can be determined by area under the ROC curve. Sensitivity and specificity at each cutoff point can be determined from ROC curve. The overall accuracy of interaction of AVC with SoV/AA was more than accuracy of the predictor parameters separately (the green line)

4.3 Discussion

In this study, AVC and aspect ratio of sinus of valsava to aortic annulus diameter as well as male gender were predictors of post-procedural PVL. We introduce AVC as the primary predictor and aspect ratio of sinus of valsava to aortic annulus as the secondary predictor of post-procedural PVL, since the accuracy of AVC in prediction of post-procedural PVL was more significant rather than aspect ratio of sinus of valsava to aortic annulus. Patients with large native SoV/AA ratio and large AVC deposition were more likely to have post-procedural PVL, especially men. Since AVC volume in men was significantly higher in compared with women's and large

amount of AVC is associated with post-procedural PVL, men are more likely to undergo PVL after TAVI procedure. Koh et al. also reported that probability of occurrence of post-procedural PVL in men is significantly higher (Koh, Lam et al. 2015). In the present study, post-procedural PVL was mostly observed in patients with highly calcified aortic valve; however PVL was not exclusively observed at the location of calcification in aortic valve cusps but was also observed at the commissures between cusps where there was no calcium lesion. Ewe et al. showed that calcification at the aortic wall and commissure with area under the ROC curve of 93% and 94% was better predictive factors for post-procedural PVL in comparison with calcification at the belly of the leaflet (Ewe, Ng et al. 2011).

Interaction of AVC with aspect ratio of sinus of valsava to aortic annulus diameter had a stronger effect on detection of PVL in comparison with AVC and SoV/AA separately. Since both SoV/AA ratio and AVC are predictors of post-procedural PVL, we recommend using interaction of these predictors to estimate whether or not post-procedural PVL occurrence is likely for a patient. The probability of PVL occurrence at different levels of interaction value can be seen in Figure 4.6. Moreover, the interaction factor has an accuracy of 91%, therefore there are errors in discriminating between patients with and without PVL at each interaction value. Those errors are defined by false positive and false negative rates. The more the model is sensitive, the better it predicts patients who will experience post-procedural PVL and the more the model is specific, the better it predicts patients who will not experience post-procedural PVL. For example at interaction value of 1330 mm^3 with 100% specificity, all patients who will not experience PVL can correctly be identified. This interaction value with sensitivity of 62% can correctly identify 62% of the patients who undergo post-procedural PVL. At interaction value of 1330 mm^3, 20% of the patients without PVL are incorrectly identified as they undergo PVL (false positive);

while, zero percent of the patients who have PVL are incorrectly identifies as not to have PVL condition (false negative).

In this study, coronary calcifications and anatomic parameters other than aspect ratio of sinus of valsava to aortic annulus were not statistically significant between patients with and without post-procedural PVL. Several previous studies also have shown the importance of role of AVC in post-TAVI aortic regurgitation (Delgado, Ng et al. 2010; John, Buellesfeld et al. 2010; Ewe, Ng et al. 2011). Ewe et al. and Koh et al. have both indicated that location and severity of aortic valve calcification are associated with location of post-procedural PVL (Ewe, Ng et al. 2011; Koh, Lam et al. 2015). In the present study, within 12 patients who had post-procedural PVL, the NCC had the highest level of AVC in 6 patients, followed by the LCC in 5 patients and RCC in 1 case. Koh et al. also reported that NCC was more calcified in majority of patients in their study, followed by LCC and RCC in less patients, respectively while, in Koh et al. report, PVL was seen at one location along the LCC in 13 patients out of 36, the RCC in 12 patients and the NCC in 11 cases. We observed at least 2 locations for PVL in each case, so the total of 30 PVL locations was observed within 10 patients in which 14 locations were at commissure between cusps and 16 locations were along each individual cusp.

Although within our small population no pattern was detected between location of AVC and location of PVL, our regression model suggested that calcifications in LCC (p-value=0.01) and RCC (p-value=0.06) were better predictors for post-procedural PVL rather than calcification in NCC. In this investigation, PVL was observed from either location of calcification in a cusp or commissure between two calcified cusps or even commissure between 2 cusps which were not severely calcified. In Koh et al. study, location of PVL corresponded with the most calcified cusp in 56% of the patients.

Location of PVL can be explained by anatomic alteration that calcification causes at the annulus area. Once the stent valve is implanted at the location of aortic valve, it pushes away the calcified leaflets towards the aortic wall. Thus, the aortic annulus or location of implanted stent becomes uneven and blood can flow back into ventricle from the gap between uneven annulus and implanted stent (Zegdi, Ciobotaru et al. 2008). In addition, calcification stiffens the valve area; the stiffness of calcified regions unbalance the movement of the aortic valve during the opening and closing. Thus, during the cardiac cycle gaps may appear between the annulus area and the implanted stent due to calcification and leads to PVL.

Several previous studies indicated that PVL is related to implantation of an undersized artificial valve into the location of native aortic valve (Jilaihawi, Kashif et al. 2012; Willson, Webb et al. 2012). For example, one of the recent studies showed that the valve calcification index which is defined as aortic root calcification volume to body surface area as well as the ratio of valve diameter to the calculated average annulus diameter (CAAD) are predictors of moderate and severe PVL (Watanabe, Lefèvre et al. 2015). Nemoto et al. also suggested that longer ascending aorta and arch are risk factors for post–procedural PVL (Nemoto, Rutten-Ramos et al. 2014). Takagi et al. indicated that the size of aortic annulus was a predictor of PVL (Takagi, Latib et al. 2011). However the relationship of anatomic characteristics of native aortic valve with post-procedural PVL was not carefully studied so far. Thus, this research found out the aspect ratio of the sinus of valsava to aortic annulus diameter of patient's native aortic valve along with AVC are independent predictors of post-procedural PVL. Therefore, by evaluating anatomic conditions of patient's aortic valve and calcification in three aortic cusps, we will be able to predict occurrence of post-procedural PVL before a patient undergoes transcatheter aortic valve implantations.

5. SUMMARY AND FUTURE WORK

5.1 Overall Summary

Aortic valve calcification is a complex mechanism that is associated with many biological, hemodynamics and anatomic factors. However, in this investigation, anatomic parameters showed statistically significant relationship with aortic valve calcification and post-procedural paravalvular leak. In Aim 1, results of our prediction model indicated that patients with large sinus of valsava and small sinotubular junction diameters are at a higher risk of developing aortic valve calcification. In Aim 2, we showed that calcification of aortic valve and aspect ratio of sinus of valsava to aortic annulus diameters are the major predictors of post-procedural paravalvular leak.

Different imaging modalities were used to visualize aortic valve calcification and dimension and to monitor valve function before and after transcatheter aortic valve implantation. Image processing methods have been developed to construct 3D models of aortic valve and calcification lesions. Comparison of 3D models with transesophageal echocardiography images determined the location of post-procedural paravalvular leak and its relation with calcification of aortic valve. Statistical analyses were performed to identify the significant difference among population and different categories. Statistical tests showed a strong correlation between calcification and anatomy of native aortic valve with risk of post-procedural paravalvular leak.

The sample size in Aim 1 and Aim 2 of this study was respectively 30 and 33 patients. Sample size is an important factor of any study in which the goal is to make inference about a population. Sample size is determined based on needs to have sufficient statistical power and the

expense of data collection. A small sample size can result in a wide confidence interval or a large risk of error. In contrast, a large sample size leads to lower error and higher precision when estimating an unknown parameter. A sample size is judged based on central limit theorem (CLT). CLT states that as sample size increases, the distribution of the mean approaches a normal distribution. Based on CLT, a sample size of 30 or more is considered large and a sample size of less than 30 is considered a small sample size. Therefore, our sample size was appropriate to make inference about the population of patients who undergo TAVI procedure.

There are several different algorithms to model a set of data. Two of the most common methods used in medical studies are linear and non-linear multivariable regressions. In linear regression, simple algebra is used to model a set of data while, in non-linear regression complicated approaches (matrix algebra) are used for data modeling. In this study, we used multiple linear regression analysis and acquired a satisfactory relationship among the variables. Due to the difficulty of non-linear regression approach, it has been suggested to use linear regression model if the curve fit of the data has a good R-squared. However, if the data cannot be appropriately modeled by linear regression method then non-linear regression method should be used.

The overall significance of this study was that bioengineering analysis of pre-procedural CT data can be utilized towards better TAVR planning as well as basic understanding of the pathogenesis of AVC. Assessing aortic valve calcification and patient-specific aortic valve anatomy allows us to design patient-specific aortic valve stents which improve valvular hemodynamic by changing the shape of the native calcified aortic valve.

5.2 Limitations and Future Work

There are a number of limitations associated with this work. For example, the CT scans for patients were acquired with different resolution and qualities; therefore different specific threshold level was applied to CT scans of each patient to segment calcification volumes in ITK-SNAP. Thus, because ITK-SNAP is not a standard clinical tool, volume measurements might have been along with some errors. Another limitation is that in this investigation several questions may remain unanswered. In order to understand the role of aortic valve anatomy in AVC and post-procedural PVL and the reason that left coronary artery becomes more calcified than right coronary artery, we need to design hemodynamics experiments to see blood flow behavior in aortic sinuses and coronary arteries for patient-specific anatomies.

The results of this investigation might be slightly different on a different population of patients. For example, in a larger population with more diversity, those factors which were known as non-significant parameters may also become statistically significant. In this study dimension of ostiums orifice and cusps were not available. Dimension of ostiums and sinuses as well as length of the leaflets might change the hemodynamics and have a role in calcification of coronary arteries and cusps, as Schäfers study found significant correlation between cusp height and clinical variable such as aortic regurgitation (Schäfers, Schmied et al. 2013), this may also affect AVC.

6. REFERENCES

Abdel-Wahab, M., R. Zahn, et al. (2011). "Aortic regurgitation after transcatheter aortic valve implantation: incidence and early outcome. Results from the German transcatheter aortic valve interventions registry." Heart 97(11): 899-906.

Aikawa, E., M. Aikawa, et al. (2009). "Arterial and aortic valve calcification abolished by elastolytic cathepsin S deficiency in chronic renal disease." Circulation 119(13): 1785-1794.

Aikawa, E., M. Nahrendorf, et al. (2007). "Osteogenesis associates with inflammation in early-stage atherosclerosis evaluated by molecular imaging in vivo." Circulation 116(24): 2841-2850.

Aikawa, M., I. Manabe, et al. (2012). "Cardiovascular inflammation." International journal of inflammation 2012.

Alwan, A. (2011). Global status report on noncommunicable diseases 2010, World Health Organization.

Balachandran, K. (2010). AORTIC VALVE MECHANOBIOLOGY–THE EFFECT OF CYCLIC STRETCH, Georgia Institute of Technology.

Balachandran, K., P. Sucosky, et al. (2009). "Elevated cyclic stretch alters matrix remodeling in aortic valve cusps: implications for degenerative aortic valve disease." American Journal of Physiology-Heart and Circulatory Physiology 296(3): H756-H764.

Balachandran, K., P. Sucosky, et al. (2011). "Hemodynamics and mechanobiology of aortic valve inflammation and calcification." International journal of inflammation 2011.

Beck, A., M. Thubrikar, et al. (2001). "Stress analysis of the aortic valve with and without the sinuses of valsalva." The Journal of heart valve disease 10(1): 1-11.

Björk, V. O. (1969). "A new tilting disc valve prosthesis." Scandinavian Cardiovascular Journal 3(1): 1-10.

Boon, A., E. Cheriex, et al. (1997). "Cardiac valve calcification: characteristics of patients with calcification of the mitral annulus or aortic valve." Heart 78(5): 472-474.

Butcher, J. T. and R. M. Nerem (2007). "Valvular endothelial cells and the mechanoregulation of valvular pathology." Philosophical Transactions of the Royal Society B: Biological Sciences 362(1484): 1445-1457.

Carapetis, J. R., A. C. Steer, et al. (2005). "The global burden of group A streptococcal diseases." The Lancet infectious diseases 5(11): 685-694.

Colli, A., R. D'Amico, et al. (2011). "Transesophageal echocardiographic scoring for transcatheter aortic valve implantation: impact of aortic cusp calcification on postoperative aortic regurgitation." The Journal of Thoracic and Cardiovascular Surgery 142(5): 1229-1235.

Dagum, P., G. R. Green, et al. (1999). "Deformational Dynamics of the Aortic Root Modes and Physiologic Determinants." Circulation 100(suppl 2): II-54-Ii-62.

Dasi, L. P., H. A. Simon, et al. (2009). "Fluid mechanics of artificial heart valves." Clinical and experimental pharmacology and physiology 36(2): 225-237.

Delgado, V., A. C. Ng, et al. (2010). "Transcatheter aortic valve implantation: role of multi-detector row computed tomography to evaluate prosthesis positioning and deployment in relation to valve function." European heart journal: ehq018.

Demer, L. L. (2001). "Cholesterol in vascular and valvular calcification." Circulation 104(16): 1881-1883.

Ewe, S. H., A. C. Ng, et al. (2011). "Location and severity of aortic valve calcium and implications for aortic regurgitation after transcatheter aortic valve implantation." The American journal of cardiology 108(10): 1470-1477.

Freeman, R. V. and C. M. Otto (2005). "Spectrum of calcific aortic valve disease pathogenesis, disease progression, and treatment strategies." Circulation 111(24): 3316-3326.

Gould, S. T., S. Srigunapalan, et al. (2013). "Hemodynamic and cellular response feedback in calcific aortic valve disease." Circulation research 113(2): 186-197.

Gripari, P., S. H. Ewe, et al. (2012). "Intraoperative 2D and 3D transoesophageal echocardiographic predictors of aortic regurgitation after transcatheter aortic valve implantation." Heart 98(16): 1229-1236.

Grünenfelder, J. and M. Y. Emmert (2015). "Aortic valve calcium score is a significant predictor for the occurrence of post-interventional paravalvular leakage after transcatheter aortic valve implantation—Results from a single center analysis of 260 consecutive patients." International journal of cardiology 181: 185-187.

Halevi, R., A. Hamdan, et al. (2015). "Progressive aortic valve calcification: Three-dimensional visualization and biomechanical analysis." Journal of biomechanics 48(3): 489-497.

Hjortnaes, J., S. E. New, et al. (2013). "Visualizing novel concepts of cardiovascular calcification." Trends in cardiovascular medicine 23(3): 71-79.

Huang, H.-Y. S., J. Liao, et al. (2007). "In-situ deformation of the aortic valve interstitial cell nucleus under diastolic loading." Journal of biomechanical engineering 129(6): 880-889.

Hufnagel, C. A. (1950). "Aortic plastic valvular prosthesis." Bulletin. Georgetown University. Medical Center 4(5): 128-130.

Iaizzo, P. A. (2009). Handbook of cardiac anatomy, physiology, and devices, Springer Science & Business Media.

Jilaihawi, H., M. Kashif, et al. (2012). "Cross-sectional computed tomographic assessment improves accuracy of aortic annular sizing for transcatheter aortic valve replacement and reduces the incidence of paravalvular aortic regurgitation." Journal of the American College of Cardiology 59(14): 1275-1286.

John, D., L. Buellesfeld, et al. (2010). "Correlation of device landing zone calcification and acute procedural success in patients undergoing transcatheter aortic valve implantations with the self-expanding CoreValve prosthesis." JACC: Cardiovascular interventions 3(2): 233-243.

Kaster, R. L., C. W. Lillehei, et al. (1970). "The Lillehei-Kaster pivoting disc aortic prosthesis and a comparative study of its pulsatile flow characteristics with four other prostheses." ASAIO Journal 16(1): 233-243.

Katz, R., N. D. Wong, et al. (2006). "Features of the metabolic syndrome and diabetes mellitus as predictors of aortic valve calcification in the Multi-Ethnic Study of Atherosclerosis." Circulation 113(17): 2113-2119.

Knight, J., V. Kurtcuoglu, et al. (2009). "Ex vivo and in vivo coronary ostial locations in humans." Surgical and radiologic anatomy 31(8): 597-604.

Kodali, S., P. Pibarot, et al. (2014). "Paravalvular regurgitation after transcatheter aortic valve replacement with the Edwards sapien valve in the PARTNER trial: characterizing patients and impact on outcomes." European heart journal: ehu384.

Koh, E. Y., K. Y. Lam, et al. (2015). "Aortic valve calcification as a predictor of location and severity of paravalvular regurgitation after transcatheter aortic valve implantation." Interactive cardiovascular and thoracic surgery 20(3): 345-350.

Lindroos, M., M. Kupari, et al. (1993). "Prevalence of aortic valve abnormalities in the elderly: an echocardiographic study of a random population sample." Journal of the American College of Cardiology 21(5): 1220-1225.

Lindroos, M., M. Kupari, et al. (1994). "Factors associated with calcific aortic valve degeneration in the elderly." European heart journal 15(7): 865-870.

Marom, G., R. Halevi, et al. (2013). "Numerical model of the aortic root and valve: optimization of graft size and sinotubular junction to annulus ratio." The Journal of Thoracic and Cardiovascular Surgery 146(5): 1227-1231.

McCarthy, J. and F. Palmer (1974). "Incidence and significance of coronary artery calcification." British heart journal 36(5): 499.

Merryman, W. D., H.-Y. S. Huang, et al. (2006). "The effects of cellular contraction on aortic valve leaflet flexural stiffness." Journal of biomechanics 39(1): 88-96.

Mirnajafi, A., J. M. Raymer, et al. (2006). "The flexural rigidity of the aortic valve leaflet in the commissural region." Journal of biomechanics 39(16): 2966-2973.

Mohler, E. R., F. Gannon, et al. (2001). "Bone formation and inflammation in cardiac valves." Circulation 103(11): 1522-1528.

Mohler III, E. R. (2004). "Mechanisms of aortic valve calcification." The American journal of cardiology 94(11): 1396-1402.

Moore, B. L. (2015). "INFLUENCE OF ANATOMIC VALVE CONDITIONS AND CORONARY FLOW ON AORTIC SINUS HEMODYNAMICS." 139.

Moore, B. L. and L. P. Dasi (2015). "Coronary Flow Impacts Aortic Leaflet Mechanics and Aortic Sinus Hemodynamics." Annals of biomedical engineering: 1-11.

Mozaffarian, D., E. J. Benjamin, et al. (2015). "Heart disease and stroke statistics-2015 update: a report from the american heart association." Circulation 131(4): e29.

Mulholland, M. W., K. D. Lillemoe, et al. (2012). Greenfield's Surgery: Scientific Principles & Practice, Lippincott Williams & Wilkins.

Nemoto, N., S. Rutten-Ramos, et al. (2014). "PARAVALVULAR LEAK AFTER TRANSCATHETER AORTIC VALVE REPLACEMENT (TAVR) IS ASSOCIATED WITH ASCENDING AORTA AND ARCH ANATOMY." Journal of the American College of Cardiology 63(12_S).

Otto, C. M. (2008). "Calcific aortic stenosis--time to look more closely at the valve." The New England journal of medicine 359(13): 1395-1398.

Pohle, K., R. Mäffert, et al. (2001). "Progression of aortic valve calcification association with coronary atherosclerosis and cardiovascular risk factors." Circulation 104(16): 1927-1932.

Possis, Z. C. (1978). Heart valve prosthesis, Google Patents.

Rajamannan, N. M., M. Subramaniam, et al. (2003). "Human aortic valve calcification is associated with an osteoblast phenotype." Circulation 107(17): 2181-2184.

Reul, H. and N. Talukder (1979). "Heart valve mechanics." Quantitative Cardiovascular Studies Clinical and Research Applications of Engineering Principles: 527-564.

Rivard, A. L., T. Bartel, et al. (2009). "Evaluation of aortic root and valve calcifications by multi-detector computed tomography." J Heart Valve Dis 18(6): 662-670.

Santos, N., J. A. De Agustín, et al. (2012). "Prosthesis/annulus discongruence assessed by three-dimensional transoesophageal echocardiography: a predictor of significant paravalvular aortic regurgitation after transcatheter aortic valve implantation." European Heart Journal-Cardiovascular Imaging: jes072.

Schäfers, H.-J., W. Schmied, et al. (2013). "Cusp height in aortic valves." The Journal of Thoracic and Cardiovascular Surgery 146(2): 269-274.

Schiffrin, E. L., M. L. Lipman, et al. (2007). "Chronic kidney disease effects on the cardiovascular system." Circulation 116(1): 85-97.

Sherif, M. A., M. Abdel-Wahab, et al. (2010). "Anatomic and procedural predictors of paravalvular aortic regurgitation after implantation of the Medtronic CoreValve bioprosthesis." Journal of the American College of Cardiology 56(20): 1623-1629.

Sorrell, V. L. and S. Kumar (2011). Doppler Contrast Echocardiography, INTECH Open Access Publisher.

Takagi, K., A. Latib, et al. (2011). "Predictors of moderate-to-severe paravalvular aortic regurgitation immediately after corevalve implantation and the impact of postdilatation." Catheterization and Cardiovascular Interventions 78(3): 432-443.

Tamburino, C., D. Capodanno, et al. (2011). "Incidence and predictors of early and late mortality after transcatheter aortic valve implantation in 663 patients with severe aortic stenosis." Circulation 123(3): 299-308.

Tops, L. F., D. A. Wood, et al. (2008). "Noninvasive evaluation of the aortic root with multislice computed tomography: implications for transcatheter aortic valve replacement." JACC: Cardiovascular Imaging 1(3): 321-330.

Watanabe, Y., T. Lefèvre, et al. (2015). "Can we predict postprocedural paravalvular leak after Edwards SAPIEN transcatheter aortic valve implantation?" Catheterization and Cardiovascular Interventions.

Willson, A. B., J. G. Webb, et al. (2012). "3-dimensional aortic annular assessment by multidetector computed tomography predicts moderate or severe paravalvular regurgitation after transcatheter aortic valve replacement: a multicenter retrospective analysis." Journal of the American College of Cardiology 59(14): 1287-1294.

Yip, C. Y. Y. and C. A. Simmons (2011). "The aortic valve microenvironment and its role in calcific aortic valve disease." Cardiovascular Pathology 20(3): 177-182.

Yoganathan, A. P., Z. He, et al. (2004). "Fluid mechanics of heart valves." Annu. Rev. Biomed. Eng. 6: 331-362.

Yushkevich, P. A., J. Piven, et al. (2006). "User-guided 3D active contour segmentation of anatomical structures: significantly improved efficiency and reliability." Neuroimage 31(3): 1116-1128.

Zarayelyan, A. (2015). "Dynamic Anatomy of Aortic Root and Its Potential Role in TAVR Prostheses Further Development and Modification." British Journal of Medicine and Medical Research 5(12): 1534-1546.

Zegdi, R., V. Ciobotaru, et al. (2008). "Is it reasonable to treat all calcified stenotic aortic valves with a valved stent?: results from a human anatomic study in adults." Journal of the American College of Cardiology 51(5): 579-584.

Zsuzsanna, S., B. Theodora, et al. (2013). "Correlations between severity of coronary calcification and impairment of Left Ventricular Ejection Fraction." Acta Medica Marisiensis 59(5): 267-269.